

(Mis-)Interpreting supernovae observations in a lumpy universe

Chris Clarkson¹, George F.R. Ellis¹, Andreas Faltenbacher²,
Roy Maartens^{2,3}, Obinna Umeh¹, and Jean-Philippe Uzan^{4,1,5}¹*Astrophysics, Cosmology & Gravity Centre, and,
Department of Mathematics & Applied Mathematics,
University of Cape Town, Cape Town 7701, South Africa*²*Physics Department, University of the Western Cape, Cape Town 7535, South Africa*³*Institute of Cosmology & Gravitation, University of Portsmouth, Portsmouth PO1 3FX, United Kingdom*⁴*Institut d'Astrophysique de Paris, UMR-7095 du CNRS,
Université Pierre et Marie Curie, 75014 Paris, France*⁵*National Institute for Theoretical Physics, Stellenbosch 7600, South Africa*

(Dated: October 29, 2018)

Light from ‘point sources’ such as supernovae is observed with a beam width of order of the sources’ size – typically less than 1 AU. Such a beam probes matter and curvature distributions that are very different from coarse-grained representations in N-body simulations or perturbation theory, which are smoothed on scales much larger than 1 AU. The beam typically travels through unclustered dark matter and hydrogen with a mean density much less than the cosmic mean, and through dark matter halos and hydrogen clouds. Using N-body simulations, as well as a Press-Schechter approach, we quantify the density probability distribution as a function of beam width and show that, even for Gpc-length beams of 500 kpc diameter, most lines of sight are significantly under-dense. From this we argue that modelling the probability distribution for AU-diameter beams is absolutely critical. Standard analyses predict a huge variance for such tiny beam sizes, and nonlinear corrections appear to be non-trivial. It is not even clear whether under-dense regions lead to dimming or brightening of sources, owing to the uncertainty in modelling the expansion rate which we show is the dominant contribution. By considering different reasonable approximations which yield very different cosmologies we argue that modelling ultra-narrow beams accurately remains a critical problem for precision cosmology. This could appear as a discordance between angular diameter and luminosity distances when comparing SN observations to BAO or CMB distances.

I. INTRODUCTION: ON NARROW BEAMS

Supernovae Ia (SNIa) observations play a critical role in the evidence for a nonzero cosmological constant (see [1] and references therein). SNIa are effective standard candles (we think their intrinsic luminosity can be calibrated from their light curve). In the standard cosmological model, their observed luminosity is used to infer their luminosity distance (or equivalently magnitude) by assuming that the geometry of the universe is well-described by a Friedmann-Lemaître (FL) background geometry that describes the universe smoothed on large scales. Of course, photons do not propagate in the geometry of a smooth FL spacetime but in the lumpy universe: a beam mostly propagates in underdense regions between clustered matter (overdense islands of matter). The problem of quantifying the effects of propagation in an inhomogeneous universe was first addressed, as far as we are aware, independently by Zel’dovich [2] and Feynman [3]. Zel’dovich introduced the empty-beam approximation to deal with light rays propagating in vacuum and this was extended to the case of a partially-filled beam by [4]. These results later came to be known as the Dyer-Roeder approximation – see below. Zel’dovich’s insight also led to other work on the problem in the 1960s [5–8].

Light propagation in inhomogeneous spacetimes gives

rise both to distortion of images and magnification of some images, because of gravitational lensing; in compensation, most images are demagnified. These effects induce, in particular, a dispersion of the observed SNIa luminosities and hence an extra scatter in the Hubble diagram [9–13]. “Precision cosmology” within the standard approach could be compromised by the effects of lensing on the interpretation of SNIa data – and thus it is crucial to characterise the magnitude of these effects precisely. A related key question is “what physical and angular sizes are relevant in estimating these effects on SNIa observations?”

A perturbative approach (i.e. with light propagating in a perturbed FL spacetime) shows that the dispersion due to large-scale structure becomes comparable to the intrinsic dispersion for redshifts $z > 1$ [14]. However, since the matter fluctuations responsible for the magnification of the SNIa also induce a shearing of the images of background galaxies, this dispersion can actually be corrected [15, 16]. A similar idea was pursued in the context of gravitational wave sirens [17]. Nevertheless, a considerable fraction of the lensing dispersion arises from sub-arcminute scales, which are not probed by shear maps smoothed on arcminute scales [18].

To estimate the dispersion induced by inhomogeneities, one first needs to determine the typical size of the

geodesic bundle associated with SNIa. The typical observational aperture is of order $1''$, whereas the beam is actually much thinner: $\mathcal{O}(1)$ AU for a source at redshift $z \sim 1$, i.e. an aperture of $\beta \sim 10^{-7}''$. This is typically smaller than the mean distance between any massive objects (galaxies, stars, H clouds, small dark matter halos) – and on a scale where the fluid continuum model may not be suitable any more. Thus the beam propagates in preferentially low density regions with rare encounters of gravitationally collapsed, high density patches (halos) resulting in highly inhomogeneous geometry.

By contrast, the standard approach implicitly uses a perturbative analysis and a fluid continuum model by treating the beam as propagating in the background and perturbed FL geometry. From this viewpoint, it is surprising that the standard analysis of SNIa data leads to a consistent result, in particular with other cosmological probes. Is a smooth cosmological model a good description of our universe, and in particular for interpreting data such as SNIa? If so, can we understand clearly why this is the case?

Standard perturbation theory reveals there are problems. If the angular diameter distance as a function of redshift in a perturbed FL model differs from the background by $\kappa(\beta)$ where β is the angular scale of observation (see below for definitions), then the variance of κ scales as,

$$\langle \kappa^2(\beta) \rangle^{1/2} \sim 10^{-2} \sigma_8 \Omega_0^{0.75} z_s^{0.8} \left(\frac{\beta}{1''} \right)^{-1-n/2}, \quad (1)$$

as derived in [19, 20], using linear perturbation theory (n is the spectral index of the power spectrum of density fluctuations and z_s the redshift of the source). This estimate was confirmed in [21] considering the nonlinear evolution of the power spectrum, but on scales below 10 arcmin, $\langle \kappa^2(\beta) \rangle$ increases more steeply than the theoretical expectation of the linear theory and is 2 to 3 times higher. Note also that (1) implies that $\langle \kappa^2(\beta) \rangle^{1/2}$ becomes of order 2×10^{-2} on an angular scale of order 1 arcmin, so that the variance becomes much larger than unity on the typical angular size of the ray bundle for SNIa. So large-scale structure induces a stochastic dispersion of the luminosity distance which is difficult to quantify with standard techniques for narrow beams. As soon as one goes down to much smaller scales, inhomogeneities also induce a systematic shift away from the background, since one cannot neglect the higher order terms. This is much more serious. The magnification of a source behaves as $\mu \sim 1 + 2\kappa + 3\kappa^2 + |\gamma|^2 + \dots$, where γ is the shear of the source (defined below), and so the mean of the magnification is $\langle \mu \rangle \sim 1 + \langle 3\kappa^2 + |\gamma|^2 \rangle + \dots \neq 1$. Thus, if the variance is large on small angular scales, we expect the overall shift to be significant – potentially of order unity or larger – on these scales too. Modelling this shift accurately is critical for interpreting SNIa observations correctly.

To estimate the effect of the inhomogeneities on smaller scales, one needs to provide a better description

of the matter distribution. Attempts to include a uniform component, high density halos and low density zones (filaments and voids) have been proposed [22, 23], but none go down to the required scale.

Narrow light bundles travel large distances ($\gtrsim 100 h^{-1} \text{Mpc}$) with a very low probability of encountering dark matter halos of substantial mass, which we quantify in the following section. The cuspy density profiles of the halos additionally reduce the probability of a bundle to cross the central, high density regions. Thus the bundles are subject mainly to Weyl focussing (i.e. induced by the gradient of the gravitational potential). These lightrays are expected to be demagnified compared to lightrays propagating in a FL spacetime of mean matter density. When one averages such ray bundles over the whole sky, this dimming is compensated by a small number of ray bundles that encounter very large density inhomogeneities, which then results in high focussing for those directions and a magnification. The general averaging argument was put forward by Weinberg [24].

A similar argument can be employed to determine the average density encountered by a light bundle from a supernova. The probability of a light bundle encountering massive halos decreases with halo mass. Massive galaxies, groups and clusters ($\gtrsim 10^{12} h^{-1} M_\odot$) are rarely encountered, yet, they comprise $\sim 50\%$ of total mass within the universe. Thus, if we measure SNIa in typical directions in the sky, we observe them in directions where the density of matter encountered by the relevant ray bundles may be expected to be less than the cosmological average (for almost all directions are of this nature). This argument does not apply to the much larger angular scales relevant to measurements of the BAO and CMB peaks. These beams do encounter sufficient matter to on average correspond to the overall cosmological density, as argued by [24]. In these circumstances, one expects not only an extra dispersion in the Hubble diagram, induced by the spatial inhomogeneity of the intervening medium, but also a systematic shift, induced by an observational selection effect, which may well be significant.

The goal of this article is to investigate these effects. We first discuss modelling the matter distribution in the real universe. Then we consider the general relativistic problem of light rays in an arbitrary spacetime, with a focus on how a light beam reacts to inhomogeneities compared to a smooth spacetime. We then consider some different approximations used to model narrow beams, such as perturbed FL models, the Dyer-Roeder approximation, as well as presenting two new approximations. Finally, we consider the problem of how Weyl focussing by many point sources is converted into Ricci focussing associated with a smooth matter distribution.

II. THE MATTER DISTRIBUTION

According to the most accepted variants of the Λ CDM paradigm gravitationally collapsed structures span a

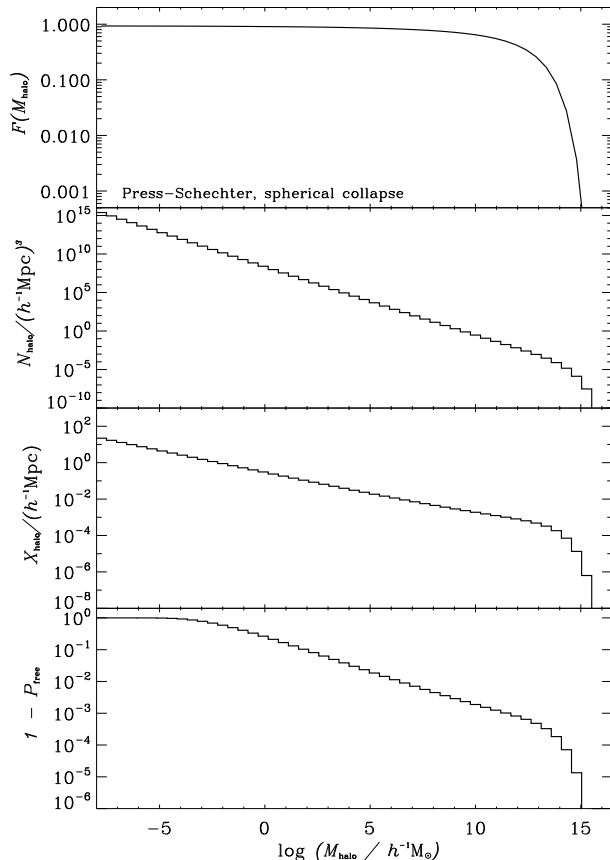


FIG. 1: The top panel shows the total fraction of cosmic mass which is locked in halos above a given mass. The Press-Schechter model predicts 50% of the total mass is locked in halos above $3 \times 10^{11} h^{-1} M_{\odot}$. The second panel gives the number of halos per mass bin per $h^{-3} \text{Mpc}^3$. The third panel displays the average number of halos per mass bin encountered by an infinitesimal thin light ray per unit length. The bottom panel indicates the probability that a ray intersects with at least one halo within a given mass bin on a distance of $1 h^{-1} \text{Mpc}$, which is equivalent to $1 - P_{\text{free}}$, where P_{free} is the probability of not hitting a halo within that mass bin on a length of $1 h^{-1} \text{Mpc}$.

mass range from $10^{-8} M_{\odot}$ (determined by the free-streaming scale of the CDM particle) to $10^{15} M_{\odot}$. In addition to the matter bound in collapsed structures a smooth component is expected which is not bound to any structure. The question we are interested in here is, how these structures affect the propagation of light bundles travelling through this inhomogeneous universe.

As first attempt to answer to this question we employ an analytic approach based on a Press-Schechter (PS) model [25]. Press and Schechter derived an analytical expression for the cumulative mass function, $F(M_{\text{halo}})$, which gives the fraction of mass locked in halos above a given mass. Integrating their formula over the whole

mass spectrum yields one. Thus the PS model predicts that *all* matter is bound in gravitationally collapsed halos, with masses ranging from zero to infinity. With the increasing dynamical range of N-body simulations, quantitative differences with this model have become apparent [26–33]. However, the difference between analytical and N-body predictions depends on the definition of a halo in the simulations. Recently, [34, 35] showed that using ‘dynamical masses’ for N-body halos yields good agreement at least for low redshifts.

The top panel of Fig. 1 shows our computation of $F(M_{\text{halo}})$ based on the 5-Year WMAP data [36]. The derivative of F determines the number density of halos, N_{halo} , as a function of mass (second panel). According to spherical collapse theory the radius of a halo with mass, M_{halo} , is given by:

$$r_{\text{halo}} = \left(\frac{3M_{\text{halo}}}{4\pi\Delta_c\rho_{\text{crit}}} \right)^{1/3} \quad (2)$$

where ρ_{crit} is the critical density of the universe and $\Delta_c = 95$ (for cosmological parameters chosen above).

The average number of halos, X_{halo} , with mass M_{halo} encountered by a single infinitesimal ray per unit length is the product of N_{halo} and the surface area of the halo.

$$X_{\text{halo}} = N_{\text{halo}}\pi r_{\text{halo}}^2 \quad (3)$$

X_{halo} is shown in the third panel from the top. The average number of halos with masses about $10^{12} h^{-1} M_{\odot}$ encountered by a light ray is ~ 0.001 . Thus, on average a single light ray of light hits one $10^{12} h^{-1} M_{\odot}$ halo every $1000 h^{-1} \text{Mpc}$.

The bottom panel displays the probability that a ray intersects with at least one halo of a given mass while travelling a distance of $1 h^{-1} \text{Mpc}$, which is equivalent to $1 - P_{\text{free}}$, where P_{free} is the probability of passing $1 h^{-1} \text{Mpc}$ freely, i.e., without encountering a single halo of that mass. To compute P_{free} we subdivide the volume into cubes with $1/N_{1D} = N_{\text{halo}}^{-1/3}$ on a side and assume that halos within a given mass bin are distributed *quasi homogeneously*, i.e., only one single halo is placed within each cube. The position of the halo within the cube is chosen randomly. With these assumptions P_{free} can be approximated by

$$P_{\text{free}} = (1 - \pi r_{\text{halo}}^2 N_{1D}^2)^{N_{1D}}. \quad (4)$$

We conclude that a light ray travelling $1 h^{-1} \text{Mpc}$ through the present, nonlinear, cosmic density field encounters with almost 100% certainty several halos with masses below $10^{-3} h^{-1} M_{\odot}$. Since the PS model does not include a smooth component the predictions for this mass range must be corrected accordingly. On the other side, the probability to hit at least one $10^{12} h^{-1} M_{\odot}$ halo is of the order of 0.1%. These results suggest we must discuss the effects of small and large scale structure on the light propagation separately.

A. Effects of small scale structure

Lensing can discriminate between a diffuse and smooth component (a gas of microscopic particles) and one of macroscopic massive objects (gravitationally bound), and has been used [37, 38] to probe the nature of dark matter on galactic scales. The two components can be characterized by a mass scale, defined by the fact that the projected density be smooth on a scale of order the angular size of the source. This gives [37]

$$M_* \sim 2 \times 10^{-23} M_\odot h^2 \left(\frac{\lambda_s}{1 \text{ AU}} \right)^3, \quad (5)$$

where λ_s is the physical size of the source.

Another important mass scale is set by the requirement that the angular size of the source, $\beta = \lambda_s/D_A(z_s)$, is smaller than the Einstein angular radius θ_E so that it can be considered as a true point source [37]:

$$M_{\text{point}} \sim 5 \times 10^{-7} M_\odot \left(\frac{\lambda_s}{1 \text{ AU}} \right)^2 \left(\frac{10^3 \text{ Mpc}}{D_A(z_s)} \right). \quad (6)$$

If $M < M_*$, the component can be considered as diffuse on the scale of the ray bundle. If $M_* < M < M_{\text{point}}$ there will be very few high magnification events with most of the lines of sight being demagnified, according to the standard lensing paradigm (see below). These two components affect the probability distribution function for the magnification. In the extreme case where the matter is composed only of macroscopic point-like objects, then most high-redshift SNIa would appear less bright than in a universe with the same density distributed smoothly, with some very rare events of magnified SNIa [37, 40, 41]. It has been argued [42] that the magnification of high-redshift SNIa can be a powerful discriminator of the nature of dark matter. In particular, based on numerical simulations, a few hundred SNIa at $z \sim 1$ could allow a 20% determination of the fraction of matter in compact objects.

The dispersion of SNIa data due to lensing has been estimated in various ways, but a complete analysis may require us to go down to scales where our knowledge of the distribution of matter is very poor. In particular, it is important to know the amount of diffuse matter compared to the amount of matter in small compact halos. Knowledge of the spatial distribution of the halos is required to determine the dispersion of the observations, keeping in mind that one also expects a bias since most lines of sight are demagnified.

The minimum mass of gravitationally bound structures is determined by the nature of the CDM particle itself. Its mass induces a free streaming scale which in turn gives rise to a mass threshold below which no gravitationally bound structure can form (in contrast to the original PS approach where there is no such cut off mass). Currently, neutralinos are the most promising CDM candidates. The lightest neutralino, with $m \sim 100 \text{ GeV}$, is

favoured, as it is both weakly interacting and stable (e.g. [43]). Its free-streaming scale is $\sim 0.7 \text{ pc}$, with a corresponding minimum halo mass $M_{\text{fs}} \sim 10^{-8} M_\odot$.

In principle, cosmological N-body simulations can be employed to determine the total amount of mass in the smooth and the halo component. Knowing the fundamental properties of the CDM particle, the initial conditions can be derived and propagated to the current epoch. However, the dynamical range required for this approach exceeds current computational resources.

One strategy to circumvent the computational limitations is to enclose a small region of very high resolution within a larger but lower resolution simulation. Using this technique [44] found that at $z = 26$ the mass function is steep, $dn(M)/dM \propto M^2$ down to M_{fs} . At that time about 5% of the mass in the high resolution region has collapsed into gravitationally bound halos (see Fig. 3 in [44]). Due to technical limitations this simulation has not been run further than $z \approx 26$.

Another strategy to determine the total mass locked in halos is via excursion set theory [45], which propagates density perturbations stochastically to generate the halo mass functions. For a Λ CDM model with 100 GeV neutralinos, 75–80% of matter is locked in halos at $z \lesssim 1$ [46]. The remaining 20–25% is smoothly distributed without being associated with any collapsed structure.

B. Effects of large scale structure

Current N-body simulations provide a very reliable picture of the cosmic large scale structure. However small scale structure can only be resolved down to the given mass resolution limit of these simulations (currently $\sim 10^8 M_\odot$). Analytical approaches, like those based on PS models, are not affected by mass resolution issues but are much more sketchy by nature. In the following we will investigate both approaches.

1. Analytical approach

Based on the PS model discussed above one can determine the probability distribution (PDF) of densities averaged along infinitesimally thin light rays. For that purpose we model the mass distribution of halos by four bins with average masses from $10^6 h^{-1} M_\odot$ to $3 \times 10^{14} h^{-1} M_\odot$. The mass bins are chosen in such a way that the one dimensional number density, N_{1D} , increases by a factor of 10 for each subsequent (decreasing) mass bin. The remaining mass contained within halos below the smallest mass bin is assumed to be homogeneously distributed. According to the PS model 15% of the total gravitational matter is found in halos below $10^6 h^{-1} M_\odot$.

The probability of a ray encountering a given total number of halos is computed as product of the various binomial coefficients and probabilities for hitting the partial number of halos per mass bin.

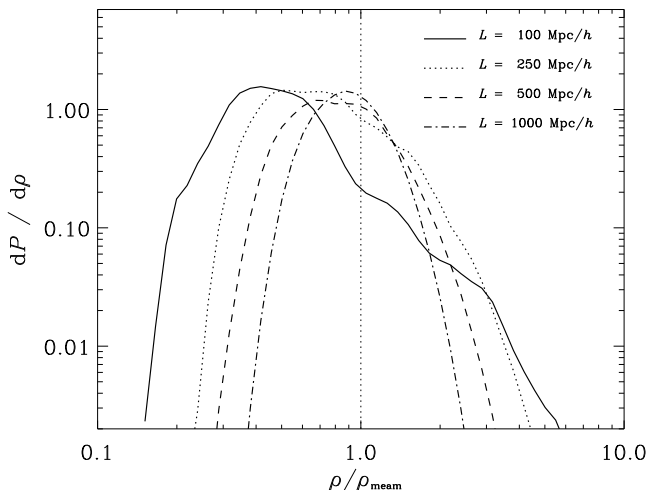


FIG. 2: Probability distribution of the averaged densities encountered by a single light ray of infinitesimal width for different path lengths based on a Press-Schechter model.

This approach allows us to compute the PDFs as a function of the path length as shown in Fig. 2. The distribution for a path length of $100 h^{-1}\text{Mpc}$ peaks at 0.4 times the mean density, ρ_{mean} . For longer path lengths the peak shifts towards ρ_{mean} . But even for a path length of $1000 h^{-1}\text{Mpc}$ (corresponding to a redshift of $z \simeq 0.25$) the distribution peaks significantly below ρ_{mean} . It is worth noting that by construction the integral of ρdP from zero to infinity equals unity. A peak below ρ_{mean} requires a high density tail for counterbalance.

The model presented here does not include halo clustering (inherent to such kind of approaches) and assumes the mass contained in objects below $10^6 h^{-1}M_{\odot}$ to be distributed smoothly (to reduce computational cost). These shortcomings let us abstain from a quantitative interpretation at this point. But we can clearly see that the majority of light rays encounters averaged densities below the mean and that the shape of the PDFs is a function of path length.

2. Numerical approach

Numerical simulations provide detailed insight into the nonlinear matter evolution inaccessible to analytical descriptions. However, they are inevitably limited in their mass resolution. The resolution is proportional to the simulation volume and inversely proportional the number of phase space elements (particles) used. For cosmological applications generally large volumes are desirable. The number of particles is limited by the available computational power. Particles of current state-of-the-art cosmological simulations have masses of a few times $10^8 M_{\odot}$. For comparison, the total mass, assuming homogeneous density distribution, contained within the volume of a light beam of 1 AU diameter and 1000 Mpc

length (corresponding to $z \approx 0.25$) is $\sim 10^{-9} M_{\odot}$.

In this section we compute the PDFs of the mean densities within long and narrow ‘beams’ based on a set of publicly available N-body simulations, namely the Bolshoi [47], the Millennium [48] and the MultiDark R1 [49] Simulation. (Descriptions of the data bases are given in [50, 51]). These simulations compute the CDM distribution within cubes of 250^3 , 500^3 and $1000^3 h^{-3}\text{Mpc}^3$ with mass resolution of 1.3×10^8 , 8.6×10^8 and $8.7 \times 10^9 h^{-1}M_{\odot}$, respectively. These mass resolutions only allow the determination of the densities within beams wider than a few tens of kpc which is many orders of magnitude larger than the expected diameter of a light beam from a supernova. Nevertheless the results derived here can give basic insight into the mean densities within the volume of the light beams from distant SNIa.

The right panel of Fig. 3 shows the PDFs of the mean densities within beams of $500 h^{-1}\text{kpc}$ diameter as a function of their length. The dashed lines based on the MultiDark simulation are shown as a consistency check. They are expected to coincide with the Bolshoi results but are more affected by Poisson noise due to the lower mass resolution. The shape of the distributions is similar to those based on the PS model (Fig. 2). Independent of length all distributions peak below the mean density. The cumulative probability for a mean density below the cosmic mean for the 100, 250, 500 and 1000 $h^{-1}\text{Mpc}$ beams is 75%, 71%, 68% and 65%, respectively. The large probability of an averaged density below cosmic mean is counterbalanced by unlikely high density encounters. Investigations based on the Millennium simulation confirm these results. The middle panel of Fig. 3 shows the PDFs for different diameters. There may be an indication that with decreasing diameters the location of the peak converges towards values close to $0.5 \times \rho_{\text{mean}}$, but we are unable to probe beam sizes below $\sim 50 h^{-1}\text{kpc}$. The shape of the distribution, and in particular that the location of the peak is below unity, is preserved independent of diameter and is expected to hold for much smaller diameters. The right hand panel of Fig. 3 displays the PDFs based on cubic volumes, i.e. the densities are measured in cubes rather than beams (left panel) while the volume remains the same. The overall shape of the PDFs is very similar to those shown on the left but the location of the peak is shifted towards smaller densities. Obviously, the geometry of the ‘test volumes’ has an impact on the PDFs. The PDFs can not be accurately determined without incorporating their spatial information of the large scale density distribution.

The picture arising from the N-body simulations is consistent with the PS model. The probability that a light beam from a supernova encounters an average density less than cosmic mean is larger than 50%. The exact value depends on light path length. With shorter distances the cumulative probability of sampling densities below cosmic mean increases. This effect may be sufficient to induce biases in the luminosity distance relation.

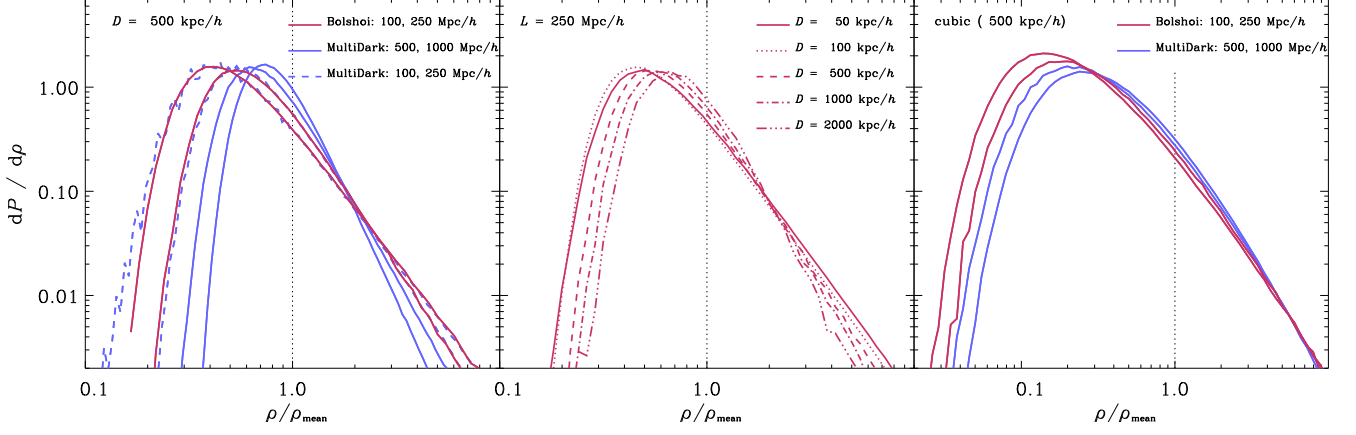


FIG. 3: Left panel: Probability distribution of averaged densities within long narrow ($0.5 h^{-1}\text{Mpc}$ diameter) beams for different path lengths using different simulations (indicated). For short path lengths (e.g., $\sim 100 h^{-1}\text{Mpc}$) most beams encounter low densities which is counterbalanced by comparatively few beams which encounter much higher densities. With increasing path length the peak of the PDF approaches the cosmic mean, but even for a beam length of $1 h^{-1}\text{Gpc}$ the peak occurs significantly below the mean density. Independent of length the average density encountered by a sufficiently large number of beams is equal to the cosmic mean density, i.e., the density weighted integrals for all curves shown above yields cosmic mean density. Middle panel: PDF for beams of the same length ($250 h^{-1}\text{Mpc}$) but different diameter (indicated). As the beam becomes narrower the PDF broadens and the location of the peak tends to shift to slightly smaller densities. Right panel: Same as left panel except here the density is measured within cubes which have the same volume as the long and narrow beams. Note the striking difference between the PDFs: the peak position and widths change when comparing tubes to cubes, and the power law tail which is prominent for beams is no longer present.

III. LIGHT PROPAGATION

From a theoretical point of view, the effects of matter inhomogeneities can be described by the geodesic deviation equation, which describes the evolution of a bundle of geodesics $x^\mu(v, s)$, where v is the affine parameter and s labels the geodesics. The past lightcones of the central observer are given by $w = \text{const}$, where w is the phase. Then $k_\mu = \partial_\mu w$, so these curves are irrotational null geodesics:

$$k^\mu k_\mu = 0, \quad k^\nu \nabla_\nu k_\mu = 0, \quad \nabla_{[\mu} k_{\nu]} = 0. \quad (7)$$

The connecting vector $\eta^\mu = dx^\mu/ds$ relates neighbouring geodesics with tangent vector $k^\mu = dx^\mu/dv$ to an arbitrary reference geodesic of the bundle, $\bar{x}^\mu(v) = x^\mu(v, 0)$, giving the distance between neighbouring geodesics and hence the physical size and shape of the bundle as one follows it down into the past. The connecting vector can always be chosen such that $k^\mu \eta_\mu = 0$ and it evolves according to the geodesic deviation equation:

$$k^\alpha k^\beta \nabla_\alpha \nabla_\beta \eta^\mu = R^\mu{}_{\nu\alpha\beta} k^\nu k^\alpha \eta^\beta. \quad (8)$$

This equation describes the change of shape of the bundle.

For fundamental observers with four-velocity u^μ

($u^\mu u_\mu = -1$), the redshift is defined by

$$1 + z(v) = \frac{(k_\mu u^\mu)_v}{(k_\mu u^\mu)_0}, \quad (9)$$

where the past-directed photon four-momentum is

$$k^\mu = (1 + z)(-u^\mu + e^\mu), \quad e^\mu u_\mu = 0, \quad e^\mu e_\mu = 1. \quad (10)$$

Here e^μ is the spatial direction of observation, and the spatial direction of propagation is $n^\mu = -e^\mu$. The affine parameter increases monotonically along each ray and coincides in an infinitesimal neighborhood of the observation point with the Euclidean distance in the rest frame of $u^\mu(0)$. Note that while it depends on the 4-velocity $u^\mu(0)$ of the observer, it does not depend on the 4-velocity $u^\mu(\bar{x}^\alpha(s))$ of the observed source.

The screen space at each point along a ray is in the observer's rest space and orthogonal to the ray direction. It is spanned by unit vectors n_a^μ ($a = 1, 2$), with $g_{\mu\nu} n_a^\mu n_b^\mu = \delta_{ab}$ and $n_a^\mu u_\mu = n_a^\mu k_\mu = 0$, that are parallel transported along the ray ($k^\mu \nabla_\mu n_a^\mu = 0$). We can choose the connecting vector to lie in the screen space, so that¹

¹ This is the Sachs basis, unique up to transformations $n_a^\mu \rightarrow r_{ab}(\alpha) n_b^\mu + p_a k^\mu$, where $r_{ab}(\alpha)$ is a rotation through angle α , and p_a are constants.

$\eta^\mu = \eta_1 n_1^\mu + \eta_2 n_2^\mu$. By (8)

$$\frac{d^2}{dv^2} \eta_a = \mathcal{R}_{ab} \eta^b, \quad (11)$$

where $\mathcal{R}_{ab} = R_{\mu\nu\alpha\beta} k^\nu k^\alpha n_a^\mu n_b^\beta$ is the screen projection of the Riemann tensor. We write

$$\mathcal{R}_{ab} = \begin{pmatrix} \Phi_{00} & 0 \\ 0 & \Phi_{00} \end{pmatrix} + \begin{pmatrix} -\text{Re } \Psi_0 & \text{Im } \Psi_0 \\ \text{Im } \Psi_0 & \text{Re } \Psi_0 \end{pmatrix} \quad (12)$$

with

$$\Phi_{00} = -\frac{1}{2} R_{\mu\nu} k^\mu k^\nu, \quad \Psi_0 = -\frac{1}{2} C_{\mu\nu\alpha\beta} m^\mu k^\nu m^\beta k^\beta, \quad (13)$$

where $m^\mu \equiv n_1^\mu - n_2^\mu$. The Einstein equations give $R_{\mu\nu} k^\mu k^\nu = 8\pi G T_{\mu\nu} k^\mu k^\nu$, where $T_{\mu\nu}$ is the total energy-momentum tensor,

$$T_{\mu\nu} = (\rho + p) u_\mu u_\nu + p g_{\mu\nu} + \pi_{\mu\nu} + q_\mu u_\nu + q_\nu u_\mu. \quad (14)$$

Here $\pi_{\mu\nu}$ is the anisotropic stress and q_μ is the momentum density. (For a perfect fluid $\pi_{\mu\nu} = 0 = q_\mu$; for more general fluids, we can always choose $q_\mu = 0$, corresponding to the frame where comoving observers see no momentum flux). Then we find

$$\Phi_{00}(v) = -4\pi G [1+z(v)]^2 (\rho + p + 2q_\mu e^\mu + \pi_{\mu\nu} e^\mu e^\nu) \Big|_{\bar{x}^\alpha(v)}. \quad (15)$$

Note that a cosmological constant Λ makes *no* contribution to Φ_{00} .

The linearity of (11) implies that

$$\eta^a(v) = \mathcal{D}^a_b(v) \frac{d\eta^b}{dv} \Big|_{v=0}, \quad (16)$$

where \mathcal{D}^a_b is the Jacobi map. By (11), we have the Jacobi matrix equation

$$\frac{d^2}{dv^2} \mathcal{D}^a_b = \mathcal{R}^a_c \mathcal{D}^c_b, \quad \eta^a(0) = 0, \quad \frac{d\mathcal{D}^a_b}{dv}(0) = \delta^a_b. \quad (17)$$

This second-order linear equation can be rewritten as a first-order nonlinear equation:

$$\frac{d}{dv} \mathcal{S}^a_b + \mathcal{S}^a_c \mathcal{S}^c_b = \mathcal{R}^a_b, \quad (18)$$

by defining the deformation matrix

$$\frac{d}{dv} \mathcal{D}^a_b = \mathcal{D}^a_c \mathcal{S}^c_b. \quad (19)$$

The Jacobi map \mathcal{D}^a_b or equivalently the deformation matrix \mathcal{S}^a_b are the central quantities to describe the distortion of the geodesic bundle. The deformation matrix is usually decomposed as²

$$\mathcal{S}^a_b = \begin{pmatrix} \hat{\theta} & 0 \\ 0 & \hat{\theta} \end{pmatrix} + \begin{pmatrix} \hat{\sigma}_1 & \hat{\sigma}_2 \\ \hat{\sigma}_2 & -\hat{\sigma}_1 \end{pmatrix}, \quad (20)$$

which defines the optical scalars $\hat{\theta}$ (null expansion) and $\hat{\sigma} \equiv \hat{\sigma}_1 + i\hat{\sigma}_2$ (null shear). These satisfy the Sachs equations [53]

$$\frac{d\hat{\theta}}{dv} + \hat{\theta}^2 + |\hat{\sigma}|^2 = \Phi_{00}, \quad (21)$$

$$\frac{d\hat{\sigma}}{dv} + 2\hat{\theta}\hat{\sigma} = \Psi_0, \quad (22)$$

$$\hat{\theta} \equiv \frac{1}{2} \nabla_\mu k^\mu, \quad |\hat{\sigma}|^2 \equiv \frac{1}{2} \nabla_\mu k_\nu \nabla^\mu k^\nu - \hat{\theta}^2. \quad (23)$$

The evolution of a ray bundle can then be discussed in terms of *Ricci* focussing (Φ_{00}) and *Weyl* focussing (Ψ_0). The first is generated by matter inside the beam [see (15)] while the second derives from matter outside the beam, which can generate a non-vanishing Weyl tensor inside the beam. This distinction leads to the problem raised by Zel'dovich [2] and Feynman [3], and posed in terms of the curvature tensor by Bertotti [5]: if the matter of the universe is clustered in massive galaxies, the bundle propagates almost exclusively in vacuum, or at least in underdense regions, and is thus mostly subject only to the Weyl focussing; by contrast, the cosmological effect is modelled using a homogeneous fluid which generates only Ricci focussing (the Weyl tensor vanishes in FL spacetime). Dyer and Roeder [54] (see also [55–57]) effectively reproduced Zel'dovich's idea and proposed an ansatz to model the propagation in regions with no intergalactic medium. Weinberg [24] disputed this model, arguing that multiple Weyl deflections by individual masses average to mimic the Ricci effect of a fluid with equal average density. Weinberg's argument, based on photon flux conservation, is effectively the basis for the standard perturbative approach – i.e. that when averaged over distances and angles, the divergence from vacuum or underdense regions is compensated by the convergence due to clumping, so that the average luminosity distance is the same as the luminosity distance in the FL background (see e.g. [58]). Weinberg's argument has been disputed [59, 60]. Later work (e.g. [61, 62]) has not produced a definitive answer to the question, in particular for the case of the very narrow beams involved in SNIa observations.

In order to properly describe a thin geodesic bundle, we need to have a good description of the matter distribution on the scales of the extension of the bundle, and determine how the effect of the inhomogeneities average during the propagation of the bundle, with two main issues in mind: (1) determining the typical amplitude of the effect and (2) understanding why the description by a smooth universe seems to provide a good description and determine its validity.

² Recall that the null rotation $\nabla_{[\mu} k_{\nu]}$ vanishes since $k_\mu = \partial_\mu w$.

A. Angular distance

The Jacobi matrix can be diagonalized by rotations:

$$\mathcal{D}^a{}_b = r(-\alpha_1) \begin{pmatrix} D_+ & 0 \\ 0 & D_- \end{pmatrix} r(\alpha_2), \quad (24)$$

where the shape parameters D_\pm are nonzero almost everywhere. Their absolute values give the semi-axes of the (elliptic) cross-section of the bundle. Once D_\pm are fixed, the angles $\alpha_{1,2}$ are unique at all points where the bundle is non-circular.

The area distance or angular diameter distance is then defined as³

$$D_A(v) = \sqrt{\det |\mathcal{D}(v)|} = \sqrt{|D_+(v)D_-(v)|}. \quad (25)$$

For a bundle converging at the observer, D_A relates the cross-sectional area A at the source to the opening solid angle at the observer. It depends on the 4-velocity of the observer, but not of the source. From (23), the null convergence is

$$\hat{\theta} = \frac{1}{\sqrt{A}} \frac{d}{dv} \sqrt{A}, \quad (26)$$

and (21) becomes

$$\frac{d^2 D_A}{dv^2} = -(|\hat{\theta}|^2 - \Phi_{00}) D_A. \quad (27)$$

For $T_{\mu\nu} k^\mu k^\nu > 0$ we have $\Phi_{00} \leq 0$ by (15), so that $|\hat{\theta}|^2 - \Phi_{00} \geq 0$. Thus

$$\frac{d^2 D_A}{dv^2} \leq 0, \quad (28)$$

in any cosmological model, as long as the null energy condition holds, irrespective of the value of the cosmological constant.

In order to compare to observations, we need the relation between v and z . We have $dz/dv = d(u^\mu k_\mu)/dv = k^\nu \nabla_\nu (u^\mu k_\mu) = k^\mu k^\nu \nabla_\nu u_\mu$. Now

$$\nabla_\mu u_\nu = \frac{1}{3} \Theta (g_{\mu\nu} + u_\mu u_\nu) + \sigma_{\mu\nu} + \omega_{\mu\nu} - u_\mu A_\nu, \quad (29)$$

where Θ is the expansion, $\sigma_{\mu\nu}$ is the shear, $\omega_{\mu\nu}$ is the vorticity and A^μ is the acceleration. In a universe containing CDM and baryons with four-velocity u^μ , and Λ (where radiation is dynamically negligible), we have $A_\mu = 0$.

By Eqs. (9) and (10), we obtain [64]

$$\frac{dz}{dv} = (1+z)^2 \left(\frac{1}{3} \Theta + \sigma_{\mu\nu} e^\mu e^\nu - A_\mu e^\mu \right). \quad (30)$$

For any quantity X evaluated along the ray bundle

$$\frac{dX}{dv} = (1+z)^2 H_\parallel(z, e^\mu) \frac{dX}{dz}, \quad (31)$$

where H_\parallel is the observed expansion rate along the line of sight [64],

$$H_\parallel(z, e^\mu) = \frac{1}{3} \Theta + \sigma_{\mu\nu} e^\mu e^\nu - A_\mu e^\mu. \quad (32)$$

The observed expansion rate is made up of an isotropic expansion monopole, an acceleration dipole and a shear quadrupole.

The set of equations (22), (27) and (30) is the basis for analyzing the effect of inhomogeneities. There are four physical effects induced by inhomogeneities that need to be taken into account:

area distance modifications due to the difference between Ricci focussing (when the rays move through a uniform medium) and Weyl focussing (due to the tidal effects of nearby matter);

redshift adjustment due to the differences between the true redshift of a source and its redshift in a smoothed out model;

affine parameter distortions since inhomogeneities change the relation $v(z)$ (this is actually where Λ affects observational relations);

displacement of the light beam since the ray path is shifted sideways by inhomogeneities and so experiences different Weyl and Ricci terms at the same v because it is at a different spacetime point.

B. Links with weak lensing formalism

The weak lensing amplification matrix \mathcal{A} relates the direction of observation,

$$\theta^a \equiv \frac{d\eta^a}{dv} \Big|_0, \quad (33)$$

to the direction of the source,

$$\theta_S^a = \frac{\eta^a(v)}{\bar{D}_A(v)} = \mathcal{A}^a{}_b \theta^b, \quad (34)$$

so that

$$\mathcal{A}^a{}_b(v) = \frac{\mathcal{D}^a{}_b(v)}{\bar{D}_A(v)}. \quad (35)$$

Here \bar{D}_A is the angular distance in a FL background, and $\bar{\mathcal{A}}^a{}_b = \delta^a_b$. We decompose \mathcal{A} into a shear (γ_1, γ_2) , a convergence κ and a rotation ω , so that

$$\mathcal{A}^a{}_b = \begin{pmatrix} 1 - \kappa - \gamma_1 & \gamma_2 - \omega \\ \gamma_2 + \omega & 1 - \kappa + \gamma_1 \end{pmatrix}. \quad (36)$$

³ Note that the terminology ‘angular diameter distance’ has two interpretations: as an area angular diameter distance, as used here, and as a linear angular diameter distance which are D_+ and D_- [68].

The magnification is given by

$$\mu \equiv \frac{S}{S_0} = \frac{1}{(1 - \kappa)^2 - |\gamma|^2 + \omega^2}, \quad (37)$$

where S, S_0 are the surface areas of the image and source ($S = S_0/\det \mathcal{A}$). Note that while \mathcal{R}_{ab} is symmetric by construction (see Eq. (11)) and \mathcal{S}_{ab} is also symmetric for a bundle converging at the observer, it is not necessarily the case for \mathcal{D}_{ab} , which actually cannot be generically symmetric; see e.g. Eq. (19).

The amplification matrix (35) and the deformation matrix (19) are both related to the Jacobi matrix, and hence they are related by

$$\bar{D}_A \frac{d}{dv} \mathcal{A}^a{}_b + \mathcal{A}^a{}_b \frac{d}{dv} \bar{D}_A = \bar{D}_A \mathcal{A}^a{}_c \mathcal{S}^c{}_b. \quad (38)$$

This implies (away from caustics, where $\det \mathcal{A} = 0$),

$$(\mathcal{A}^{-1})^a{}_c (\mathcal{A}^c{}_b)' + \delta_b^a \frac{\bar{D}'_A}{\bar{D}_A} = \mathcal{S}^a{}_b, \quad (39)$$

with a prime denoting $\partial/\partial v$ and where

$$(\mathcal{A}^{-1})^a{}_b = \mu \begin{pmatrix} 1 - \kappa + \gamma_1 & -\gamma_2 + \omega \\ -\gamma_2 - \omega & 1 - \kappa - \gamma_1 \end{pmatrix}. \quad (40)$$

The Sachs optical scalars are then given by

$$\hat{\theta} = \left(\ln \frac{D_A}{\sqrt{\mu}} \right)' \quad (41)$$

$$\hat{\sigma}_1 = -\mu [(1 - \kappa)\gamma_1' + \gamma_1\kappa' + \gamma_2\omega' - \omega\gamma_2'], \quad (42)$$

$$\hat{\sigma}_2 = \mu [(1 - \kappa)\gamma_2' + \gamma_2\kappa' - \gamma_1\omega' + \omega\gamma_1'], \quad (43)$$

with the constraint that $\omega\gamma_2' - \gamma_2\omega' = (1 - \kappa)\gamma_1' - \gamma_1\kappa'$ that arises from $\nabla_{[\mu} k_{\nu]} = 0$. These relations are useful since the optical scalars are more general (they are defined for any spacetime geometry), while the weak lensing scalars are widely used in cosmology (but they assume a FL background, see Ref. [63] for a general description). While generically $\omega \neq 0$, one can see that these equations imply that for a FL spacetime only $\hat{\theta} = D'_A/D_A$ is non-vanishing at the background level while the shear appears only at linear order in perturbation and one has $(\hat{\sigma}_1, \hat{\sigma}_2) = (-\gamma_1, \gamma_2)$ and the rotation appears only at second order in perturbations.

C. From affine parameter to redshift dependence

The evolution equations (22), (27) for the null shear and angular distance are in terms of the unobservable affine parameter v . We need to convert to the observed redshift, using (30). Using (31), we obtain

$$\begin{aligned} \frac{d^2 z}{dv^2} &= k^\mu k^\nu k^\alpha \nabla_\mu \nabla_\nu u_\alpha \\ &= -\frac{2}{3}(1+z)^3 H_\parallel \Theta - \frac{1}{3}(1+z)^3 k^\alpha \nabla_\alpha \Theta \\ &+ (1+z) k^\mu k^\alpha \nabla_\alpha A_\nu + (1+z)^2 H_\parallel k^\nu A_\nu \\ &- k^\mu k^\nu k^\alpha \nabla_\alpha \sigma_{\mu\nu}. \end{aligned} \quad (44)$$

The last term can be evaluated by expanding k^α with (10) and using $u^\nu u^\alpha \nabla \sigma_{\mu\nu} = -\sigma_{\mu\nu} A^\nu$ and $u^\nu e^\alpha \nabla \sigma_{\mu\nu} = -\sigma_{\mu\nu} e^\alpha \nabla_\alpha u^\nu$. It follows that for any quantity X ,

$$\frac{d^2 X}{dv^2} = (1+z)^4 H_\parallel^2 \frac{d^2 X}{dz^2} + (1+z)^3 Q \frac{dX}{dz}, \quad (45)$$

where

$$\begin{aligned} Q &= \frac{2}{3} \Theta H_\parallel - \frac{1}{3} \dot{\Theta} + A_\mu A^\mu \\ &+ e^\mu \left(-\frac{1}{3} \nabla_\mu \Theta + H_\parallel A_\mu - \dot{A}_\mu - u^\nu \nabla_\mu A_\nu + 2\sigma_{\mu\nu} A^\nu \right) \\ &+ e^\mu e^\nu \left(\frac{2}{3} \Theta \sigma_{\mu\nu} - \dot{\sigma}_{\mu\nu} - 2\sigma_\mu{}^\alpha \sigma_{\alpha\nu} - 2\omega_\mu{}^\alpha \omega_{\alpha\nu} \right. \\ &\left. + \nabla_\mu A_\nu \right) - e^\alpha e^\nu e^\mu \nabla_\alpha \sigma_{\mu\nu}. \end{aligned} \quad (46)$$

This form of Q is completely general, for any space-time geometry and energy-momentum tensor, and independent of the field equations. It is convenient to write H_\parallel^2 and Q in terms of covariant multipoles, using a covariant generalization of a spherical harmonic expansion [64]. We expand in terms of the trace-free products $e^{\langle\mu} e^{\nu\rangle}$, $e^{\langle\mu} e^\nu e^{\alpha\rangle}$ and $e^{\langle\mu} e^\nu e^\alpha e^{\beta\rangle}$, and use the spatial covariant derivative $\tilde{\nabla}_\mu$. Then we obtain [65]:

$$\begin{aligned} H_\parallel^2 &= \frac{1}{9} \Theta^2 + \frac{1}{3} A_\mu A^\mu + \frac{2}{15} \sigma_{\mu\nu} \sigma^{\mu\nu} \\ &- e^\mu \left[\frac{2}{3} \Theta A_\mu + \frac{4}{5} A^\nu \sigma_{\mu\nu} \right] \\ &+ e^{\langle\mu} e^{\nu\rangle} \left[A_\mu A_\nu + \frac{2}{3} \Theta \sigma_{\mu\nu} + \frac{4}{7} \sigma^\alpha{}_\mu \sigma_{\nu\alpha} \right] \\ &- 2e^{\langle\mu} e^\nu e^{\alpha\rangle} A_\mu \sigma_{\nu\alpha} + e^{\langle\mu} e^\nu e^\alpha e^{\beta\rangle} \sigma_{\mu\nu} \sigma_{\alpha\beta}, \end{aligned} \quad (47)$$

and

$$\begin{aligned} Q &= \frac{4\pi G}{3} (\rho + 3p) - \frac{1}{3} \Lambda + \frac{1}{3} \Theta^2 + \sigma_{\mu\nu} \sigma^{\mu\nu} \\ &- \frac{1}{3} \omega_{\mu\nu} \omega^{\mu\nu} + A_\mu A^\mu - \frac{2}{3} \tilde{\nabla}^\mu A_\mu \\ &+ e^\mu \left[\frac{1}{3} \tilde{\nabla}_\mu \Theta + \frac{2}{5} \tilde{\nabla}^\nu \sigma_{\mu\nu} \right. \\ &\left. + \dot{A}_\mu - \frac{4}{3} \Theta A_\mu - \frac{17}{5} A^\nu \sigma_{\mu\nu} - A^\nu \omega_{\mu\nu} \right] \\ &+ e^{\langle\mu} e^{\nu\rangle} \left[E_{\mu\nu} - 4\pi G \pi_{\mu\nu} + 2\Theta \sigma_{\mu\nu} + 3\sigma^\alpha{}_\mu \sigma_{\nu\alpha} \right. \\ &\left. + \omega_\mu{}^\alpha \omega_{\alpha\nu} + 2\omega_{\alpha\mu} \sigma_\nu{}^\alpha - 2\tilde{\nabla}_\mu A_\nu \right] \\ &+ e^{\langle\mu} e^\nu e^{\alpha\rangle} \left[\tilde{\nabla}_\mu \sigma_{\nu\alpha} - A_\mu \sigma_{\nu\alpha} \right] \end{aligned} \quad (48)$$

where we also used the covariant evolution and constraint equations of GR (see [66]). Here $E_{\mu\nu} = C_{\mu\alpha\nu\beta} u^\alpha u^\beta$ is the electric part of the Weyl tensor (generalizing the Newtonian tidal tensor). These expressions show clearly the covariant monopole and higher multipoles; for example,

the octupole of Q is $\tilde{\nabla}_{\langle\mu}\sigma_{\nu\alpha\rangle} - A_{\langle\mu}\sigma_{\nu\alpha\rangle}$. Note that the monopole of H_{\parallel}^2 has contributions from the shear even though the monopole of H_{\parallel} does not.

Finally we can rewrite the evolution equation (27) for the angular distance in terms of redshift:

$$(1+z)^2 H_{\parallel}^2 \frac{d^2 D_A}{dz^2} + (1+z) Q \frac{dD_A}{dz} = - \left[4\pi G \left(\rho + p + 2q_{\mu} e^{\mu} + \pi_{\mu\nu} e^{\mu} e^{\nu} \right) + \frac{|\hat{\sigma}|^2}{(1+z)^2} \right] D_A. \quad (49)$$

This is a completely general and nonlinear equation, valid in any spacetime, with any matter content, where H_{\parallel}^2 and Q are given by (47) and (48). The null shear terms are given by the remaining Sachs equation (22); in terms of redshift, this is

$$H_{\parallel} \left(\frac{d\hat{\sigma}_a}{dz} + \frac{1}{D_A} \frac{dD_A}{dz} \hat{\sigma}_a \right) = - (E_{\mu\nu} - \varepsilon_{\mu\alpha\beta} e^{\alpha} H_{\nu}^{\beta}) N_a^{\mu\nu}, \quad (50)$$

$$N_a^{\mu\nu} \equiv (n_1^{\mu} n_1^{\nu} - n_2^{\mu} n_2^{\nu}, n_1^{\mu} n_2^{\nu} + n_2^{\mu} n_1^{\nu}), \quad (51)$$

where $H_{\mu\nu} = \frac{1}{2} \varepsilon_{\mu\alpha\beta} C^{\alpha\beta}{}_{\nu\kappa} u^{\kappa}$ is the magnetic part of the Weyl tensor – which has no Newtonian analogue – and $\varepsilon_{\mu\nu\alpha}$ is the spatial alternating tensor.

Equations (49) and (50) form a closed system that determines D_A and $\hat{\sigma}$ in terms of z and e^{μ} . In particular, we see what is required to determine D_A in a lumpy universe: the total energy-momentum tensor (i.e. $\rho, p, q_{\mu}, \pi_{\mu\nu}$), the kinematics of the fundamental four-velocity (i.e. $\Theta, \sigma_{\mu\nu}, \omega_{\mu\nu}, A_{\mu}$), the magnetic and electric part of the Weyl tensor, $H_{\mu\nu}$ and $E_{\mu\nu}$.

In a universe with dust matter (CDM and baryons, sharing the same four-velocity), with dark energy in the form of Λ and where we can neglect radiation (i.e. at late times), we have

$$p = A_{\mu} = q_{\mu} = \pi_{\mu\nu} = 0. \quad (52)$$

From now on we will make this assumption, together with $\omega_{\mu\nu} = 0$. Then H_{\parallel}^2 and Q simplify to

$$H_{\parallel}^2 = \frac{1}{9} \Theta^2 + \frac{2}{15} \sigma_{\mu\nu} \sigma^{\mu\nu} + e^{\langle\mu} e^{\nu\rangle} \left[\frac{2}{3} \Theta \sigma_{\mu\nu} + \frac{4}{7} \sigma^{\alpha}{}_{\mu} \sigma_{\nu\alpha} \right] + e^{\langle\mu} e^{\nu} e^{\alpha} e^{\beta\rangle} \sigma_{\mu\nu} \sigma_{\alpha\beta}, \quad (53)$$

$$Q = \frac{4\pi G}{3} \rho - \frac{1}{3} \Lambda + \frac{1}{3} \Theta^2 + \sigma_{\mu\nu} \sigma^{\mu\nu} + e^{\mu} \left[\frac{1}{3} \tilde{\nabla}_{\mu} \Theta + \frac{2}{5} \tilde{\nabla}^{\nu} \sigma_{\mu\nu} \right] + e^{\langle\mu} e^{\nu\rangle} \left[E_{\mu\nu} + 2\Theta \sigma_{\mu\nu} + 3\sigma^{\alpha}{}_{\mu} \sigma_{\nu\alpha} \right] + e^{\langle\mu} e^{\nu} e^{\alpha\rangle} \tilde{\nabla}_{\mu} \sigma_{\nu\alpha}, \quad (54)$$

and the angular distance equation (49) becomes

$$(1+z)^2 H_{\parallel}^2 \frac{d^2 D_A}{dz^2} + (1+z) Q \frac{dD_A}{dz} = - \left[4\pi G \rho + \frac{|\hat{\sigma}|^2}{(1+z)^2} \right] D_A. \quad (55)$$

The form of (50) is unchanged.

IV. MODELS BASED ON DIFFERENT APPROXIMATIONS

We briefly review the standard FL approach and the DR approximation, and then we propose and investigate modifications of the DR model. (For other related reviews, see also [67–70].) The set of equations (21), (22) and (30) – equivalently (49) and (50) – is completely general and does not depend on the choice of a particular spacetime geometry. We show here how they lead to different expressions for the angular distance as a function of redshift, depending on the assumptions on the distribution of the matter.

A. Smooth FL model

If we assume the matter is smoothly distributed, then the universe can be described by a FL geometry,

$$ds^2 = a^2(\eta) [-d\eta^2 + d\chi^2 + f_K^2(\chi) d\Omega^2], \quad (56)$$

$$H(z) = H_0 \sqrt{\Omega_{m0}(1+z)^3 + \Omega_{\Lambda 0} + \Omega_{K0}(1+z)^2} \quad (57)$$

where $f_K(\chi) = \sin(\sqrt{K}\chi)/\sqrt{K}$ is the comoving angular distance. The Weyl tensor vanishes, so that $\Psi_0 = 0$, and $\hat{\sigma} = 0$ by (23), consistent with (22). Also, $\mathcal{R}_a^b = \Phi_{00} \delta_a^b$, and $H_{\parallel} = H$ by (31). Then using (15), it follows that (49) reduces to

$$\frac{d^2 \bar{D}_A}{dz^2} + \left(\frac{d \ln H}{dz} + \frac{2}{1+z} \right) \frac{d \bar{D}_A}{dz} = - \frac{3}{2} \Omega_{m0} \frac{H_0^2}{H^2} (1+z) \bar{D}_A. \quad (58)$$

It is important to realize that $H(z)$ in this equation appears from the change of variable from v to z .

This equation also follows directly from the Jacobi matrix equation (17), which is easily solved after a conformal transformation,

$$\frac{d^2}{d\tilde{v}^2} \mathcal{D}_b^a = -K \mathcal{D}_b^a, \quad (59)$$

where \tilde{v} is the affine parameter in the conformal spacetime of the static metric $d\tilde{s}^2 = -d\eta^2 + f_K^2(\chi) d\Omega^2$. The solution of (59) is $\mathcal{D}_b^a = f_K(\tilde{v}) \delta_b^a$. One can choose \tilde{v} either as η or χ and the angular distance is then given by the standard formula [71–73]

$$\bar{D}_A(z) = \frac{a_0}{(1+z)} f_K[\chi(z)]. \quad (60)$$

Along the past lightcone $d\chi = -d\eta$ and $dz/d\eta = -a_0 H(z)$, so that

$$a_0 H_0 \chi(z) = \int_0^z \frac{dz'}{H(z')/H_0}. \quad (61)$$

Since $d\chi = dz/H$, (59) recovers (58), after using $\dot{H} = -(1+z)HdH/dz$ and the Einstein equation for \dot{H} . We can either solve (59) or (58) but the first is more direct. Also, the derivation of (58) required the relation $v(z)$, or equivalently $\tilde{v}(z)$.

For a FL universe $\mathcal{A}_b^a = \delta_b^a$ (i.e. $\kappa = \gamma_1 = \gamma_2 = 0$) and then $\mathcal{S}_b^a = (\dot{f}_K/f_K)\delta_b^a$, so that only $\hat{\theta} = f_K^{-1}df_K/d\tilde{v}$ is non-vanishing, which is a consequence of the spatial homogeneity and isotropy. After integration of (22), $\sqrt{A} = f_K$ in the conformal spacetime, so that again we recover the same expression for the angular distance.

B. Perturbed FL model

The simplest way to account for inhomogeneous matter is via perturbation theory. At first order for scalar perturbations,

$$ds^2 = a^2(\eta) [-(1+2\Phi)d\eta^2 + (1-2\Psi)\gamma_{ij}dx^i dx^j], \quad (62)$$

in Newtonian gauge, where Φ and Ψ are the Bardeen potentials. The angular distance is

$$D_A = \bar{D}_A(1 + \delta_A), \quad (63)$$

and the distance duality relation implies that the luminosity distance is $D_L = (1+z)^2 \bar{D}_A(1 + \delta_A)$. Thus

$$\delta_L(z, \mathbf{n}) = \delta_A(z, \mathbf{n}) + 2 \frac{\delta z(z, \mathbf{n})}{(1+z)^2}, \quad (64)$$

where \mathbf{n} is the direction of observation. The second term encodes fluctuations of photon energy due to the local gravitational potentials as well as Doppler effects, and is similar to the Sachs-Wolfe effect on the CMB. It was investigated in [74] and also estimated in [75] in another context, but neglected in [15, 16, 76–79], which assumed $\delta_L = \delta_A$.

As long as the bundle remains in the weak lensing regime,

$$\mu \simeq 1 + 2\kappa, \quad (65)$$

so that $\delta_L(z, \mathbf{n}) = -\kappa(z, \mathbf{n})$. This assumes that the inhomogeneities can be described by density fluctuations of a *homogeneous* field. Then δ_L is a stochastic field of zero mean, so that $\langle \mu \rangle = 1$ (in terms of ensemble average) and thus $\langle D_A(z, \mathbf{n}) \rangle = \bar{D}_A(z)$. In such a description, the FL angular distance is the mean distance that a collection of observers will determine. There may indeed be a bias from this prediction arising from our actual position in the universe. This is a cosmic variance problem.

1. Derivation from the Jacobi map equation

The Jacobi equation (59) reduces to

$$\frac{d^2}{d\tilde{v}^2} \mathcal{D}_{ab}^{(1)} + K \mathcal{D}_{ab}^{(1)} = f_K(\tilde{v}) \mathcal{R}_{ab}^{(1)}(\tilde{v}), \quad (66)$$

where $\mathcal{D}_{ab} = \mathcal{D}_{ab}^{(0)} + \mathcal{D}_{ab}^{(1)}$, and $\mathcal{D}_{ab}^{(0)} = f_K(\tilde{v})\delta_{ab}$ is the background Jacobi matrix derived above. This equation has the integral solution

$$\mathcal{D}_{ab}^{(1)}(\tilde{v}) = \int_0^{\tilde{v}} f_K(\tilde{v}') f_K(\tilde{v} - \tilde{v}') \mathcal{R}_{ab}^{(1)}(\tilde{v}') d\tilde{v}', \quad (67)$$

so that the amplification matrix is given by

$$\mathcal{A}_{ab}^{(1)}(v) = \int_0^v \frac{f_K(v') f_K(v - v')}{f_K(v)} \mathcal{R}_{ab}^{(1)}(v') dv', \quad (68)$$

where $2\mathcal{R}_{ab}^{(1)} = \delta g_{\mu\nu, \alpha\beta} k^\mu k^\nu n_a^\alpha n_b^\beta$. Since we are interested in modes smaller than the Hubble scale, we assume that the spatial curvature does not influence the perturbations and neglect it in the computation of $\mathcal{R}_{ab}^{(1)}$ while we keep it in the geometrical factors. We find $\mathcal{R}_{ab}^{(1)} = -\partial_a \partial_b (\Phi + \Psi) = -2\partial_a \partial_b \Phi$, where $\Psi = \Phi$ since we can neglect anisotropic stress at late times and on sub-Hubble scales. Then the amplification matrix is $\mathcal{A}_{ab} = \delta_{ab} - \partial_a \partial_b \psi(\mathbf{n}, \chi)$ with

$$\psi \equiv 2 \int_0^\chi \frac{f_K(\chi') f_K(\chi - \chi')}{f_K(\chi)} \Phi[f_K(\chi') \mathbf{n}, \chi'] d\chi'. \quad (69)$$

We conclude that $\delta_A = -\kappa$ with

$$\delta_A = -\kappa(\mathbf{n}, \chi) = -\frac{3}{2} H_0^2 \Omega_{m0} \times \int \frac{f_K(\chi') f_K(\chi - \chi')}{f_K(\chi)} \frac{\delta[f_K(\chi') \mathbf{n}, \chi']}{a(\chi')} d\chi', \quad (70)$$

where the Poisson equation has been used to replace $\nabla^2 \Phi$ with δ . This gives the fluctuation of the angular distance in the direction \mathbf{n} , taking into account propagation in a perturbed spacetime.

2. Derivation from the Sachs equations

The same result can, in principle, be derived from the Sachs equations (21), (22) and (30). The background and first order equations are:

$$D_A^{(0)''} = \Phi_{00}^{(0)} D_A^{(0)}, \quad (71)$$

$$z^{(0)'} = \frac{1}{3} [1 + z^{(0)}]^2 \Theta^{(0)}, \quad (72)$$

$$D_A^{(1)''} = \Phi_{00}^{(0)} D_A^{(1)} + D_A^{(0)} \Phi_{00}^{(1)}, \quad (73)$$

$$z^{(1)'} = \frac{2}{3} [1 + z^{(0)}] \Theta^{(0)} z^{(1)} \quad (74)$$

$$+ [1 + z^{(0)}]^2 \left[\frac{1}{3} \Theta^{(1)} + \sigma_{\mu\nu}^{(1)} e_{(0)}^\mu e_{(0)}^\nu \right], \quad (75)$$

$$\hat{\sigma}^{(1)'} + 2\hat{\theta}^{(0)} \hat{\sigma}^{(1)} = \Psi_0^{(1)}, \quad (76)$$

$$\delta_L = \delta_A + 2 \frac{z^{(1)}}{1 + z^{(0)}}, \quad (77)$$

where primes are $\partial/\partial v$.

By (30) with $H_{\parallel} = H$, (72) reduces to the definition $H = \dot{a}/a$, and then (71) can be integrated to give (60). Then (73) is similar to (66), with the source term given by

$$\Phi_{00}^{(1)} = -4\pi G\rho^{(0)} \left[1 + z^{(0)} \right]^2 \left[\frac{\rho^{(1)}}{\rho^{(0)}} + 2 \frac{z^{(1)}}{1 + z^{(0)}} \right]. \quad (78)$$

Since $\hat{\theta}^{(0)}$ is known, (76) can be integrated once the source (which depends on gradients of the gravitational potentials) is known.

These two derivations have to give the same answer, which they actually do if the effect of perturbations is not neglected in any of the equations, and in particular in the equation for $v(z)$.

C. Dyer–Roeder approximation

It is important to stress that the perturbative description still assumes that the distribution of matter is continuous (i.e. it assumes that the fluid approximation holds on the scale of interest), so that, as long as one is in the weak lensing regime, the whole effect arises from Ricci focusing with the density of matter equal to the average cosmic density (because the effect of the shear appears only at second order). Zel’dovich [2] pointed out that light is actually more likely to propagate in underdense regions so that an overall demagnification was expected. This idea was followed up by [4–8]. The approach came to be named after the later work of Dyer and Roeder [54–56].

The main assumptions of the DR approximation are: (1) the Sachs equation (22) holds; (2) the relation $v(z)$ is the FL one, (30) with $H_{\parallel} = H$; (3) the null shear $\hat{\sigma}$ vanishes, as in a FL universe; (4) Φ_{00} is replaced by $\alpha(z)\Phi_{00}$, where $\alpha(z)$ represents the fraction of (the mean) matter intercepted by the geodesic bundle. In summary, the DR model assumes that the bundle is propagating in a FL universe but that the Ricci focusing is reduced (to reproduce the fact that the beam propagates mostly in vacuum or underdense regions) and the Weyl focusing remains zero. This implies that the DR equation is

$$\begin{aligned} \frac{d^2 \bar{D}_A}{dz^2} + \left(\frac{d \ln H}{dz} + \frac{2}{1+z} \right) \frac{d \bar{D}_A}{dz} \\ = -\frac{3}{2} \Omega_{m0} \frac{H_0^2}{H^2} (1+z) \alpha(z) \bar{D}_A. \end{aligned} \quad (79)$$

This attempts to model the global effect of inhomogeneity in a “mean way”, while still assuming that the universe is isotropic and homogeneous. The consistency of the DR approximations has been questioned by Ehlers and Schneider [81] and others (e.g. [67–69]), independently of Weinberg’s photon flux conservation argument [24].

The smoothness parameter α was initially assumed to be constant [54–56]. Later it was refined to take into account its redshift dependence due to the growth of structure [82–84] and then related to the statistical properties

of large-scale structure [69, 85]. A novel use of the DR approach was proposed in [11, 12] to correct SNIa observations for the matter distribution along the line of sight, which has important implications for parameter estimation [86].

On large scales (Mpc) we expect a distribution of 3D compensated voids giving partially 1D compensated matter distributions along the line of sight [85]. The lensing effects will not be the same as a smooth distribution of matter. On smaller scales (2 kpc to 1 A.U.) we expect to mainly move through voids, contaminated by remnant baryonic gas and non-baryonic dark matter, plus the nearly-smoothly distributed photons and neutrinos. This suggests that the effect can be significant if matter is clustered on small scales with most of the light beams used in SNIa observations preferentially moving through voids.

D. Modifying the DR approximation

The previous discussions make it explicit that the DR approximation is not a satisfactory model for the effects of clumping on ray bundles. Consider the $D_A(z)$ equation, in the absence of pressure and null shear:

$$\begin{aligned} H_{\parallel}(z) \frac{d}{dz} \left[(1+z)^2 H_{\parallel}(z) \frac{d}{dz} D_A(z) \right] \\ = -4\pi G\rho(z) D_A(z), \end{aligned} \quad (80)$$

where $H_{\parallel}(z) = \Theta/3 + \sigma_{\mu\nu} e^{\mu} e^{\nu}$. The DR approximation assumes that we can model the encounters of photons with inhomogeneous matter, and not a homogeneous background spacetime, by using $\rho(z)$ as the “true” density along a ray – while leaving the rest of the equation as in the smooth background. Another way to think of this is that the relationship between the affine parameter and redshift is held smooth, and inhomogeneities are assumed not to affect the $v(z)$ relation significantly. However, photons only experience the local curvature, shear and expansion and the average FL-behaviour must somehow emerge from integration along the line of sight.

As discussed above, even in the perturbed FL case the relation $v(z)$ fluctuates, and so the DR relation cannot be relied upon as a useful approximation even in that situation. In particular, α must depend on the line of sight since each bundle experiences a different matter profile. In a more general sense, the DR approximation does not account for changes in the local expansion rate due to clumping [69], and does not capture the essence of weak lensing unless $\alpha(z)$ is tuned to a specific form, with no apparent physical motivation [85].

We do not aim to provide a detailed analysis of the DR model here. Rather we offer some possible alternatives in order to estimate how significant the effect of clumping could be, as well as to show how difficult it is to model in a simple but reliable way.

1. Modified DR

In a universe with irrotational dust and arbitrary inhomogeneity, the generalized Friedmann equation is [66]

$$\frac{1}{3}\Theta^2 = 8\pi G\rho + \Lambda + \frac{1}{2}\sigma_{\mu\nu}\sigma^{\mu\nu} - \frac{1}{2}\mathcal{R}, \quad (81)$$

where \mathcal{R} is the Ricci curvature scalar of the 3-surfaces orthogonal to the matter four-velocity. By holding Θ fixed to the FL background value $3H$, the DR approximation effectively assumes that the variations of ρ on any null geodesic are compensated by corresponding fluctuations in the shear and curvature, which seems unphysical.

We expect a photon in the real universe to react to the nonlocal part of the gravitational field created by dark matter halos through local curvature fluctuations in addition to the dynamics of the matter in the intervening space. A reasonable alternative to DR, then, is to first write out the $D_A(z)$ equation in a general FL model, using the Friedmann equation to evaluate dH/dz . Substituting for $H(z)$ using (57) everywhere, we see that Ω_m appears in several places. Then, replacing $\rho_m \rightarrow \alpha\rho_m$ gives a plausible alternative to the usual DR approximation:

$$\begin{aligned} \frac{d^2\bar{D}_A}{dz^2} + \left\{ \frac{(1+z)H_0}{2\tilde{H}^2} [3\alpha(z)\Omega_{m0}(1+z) + \Omega_{K0}] \right. \\ \left. + \frac{2}{1+z} \right\} \frac{d\bar{D}_A}{dz} = -\frac{3}{2}\Omega_{m0}\frac{H_0^2}{\tilde{H}^2}(1+z)\alpha(z)\bar{D}_A \end{aligned} \quad (82)$$

where

$$\tilde{H}(z)^2 = H_0^2 [\alpha(z)\Omega_{m0}(1+z)^3 + \Omega_{\Lambda0} + \Omega_{K0}(1+z)^2] \quad (83)$$

This modified DR equation attempts to take into account some aspects of the change in expansion expected from an inhomogeneous matter distribution. There are clearly a variety of ways to do this (e.g., we have ignored $\alpha_{,z}$ terms which could be important), but we have chosen just one. See [87] for an alternative approach.

2. Shell approximation

Consider a single line of sight, smoothed over some scale λ . The density profile along this line of sight takes some form $\rho_\lambda(z)$. If we neglect the angular part of the shear $\sigma_{\mu\nu}$, then we can think of the beam as passing through shells of differing density. There exists a spherically symmetric Lemaître-Tolman-Bondi (LTB) model with non-zero Λ that has the same density profile $\rho_\lambda(z)$ along the past lightcone from the centre. The $D_A(z)$ relation in the LTB model viewed from the centre will approximate the $D_A(z)$ relation along the line of sight we are trying to model. Each line of sight would have a different associated LTB model (a mosaic of cones around

us, in the language of [11]). The utility of this approximation lies in the fact that we can specify a density profile on a surface of constant time, and use the exact LTB solution to evolve the density backwards onto the past lightcone. We can then calculate $D_A(z)$ exactly for that line of sight. Most importantly, this will account for the variable expansion rate along the direction of propagation which also takes into account the radial component of the shear.

In the LTB model, the angular Hubble rate is given by an effective Friedmann equation [88]

$$\frac{H_\perp^2(t, r)}{H_{\perp0}^2(r)} = \Omega_{m0}(r) a_\perp^{-3} + \Omega_{K0}(r) a_\perp^{-2} + \Omega_{\Lambda0}(r), \quad (84)$$

where the angular scale factor $a_\perp(t, r)$ is normalized to unity today, the Ω 's have an arbitrary radial degree of freedom in them, and $H_{\perp0}(r)$ is calculated once the age is set (or the Hubble rate at the centre is chosen). If Ω_{m0} is chosen as a constant we have an FL model. To model a radial line of sight we can choose the density profile today as $\rho_0(r) = [1 + \delta(r)]\rho_\lambda(0)$, and then

$$\Omega_{m0}(r) = \frac{1}{H_{\perp0}^2(r)} \int_0^r dr' r'^2 \rho_0(r'). \quad (85)$$

Then (84) evolves the density back onto the past lightcone, using

$$\frac{dt}{dz} = -\frac{1}{(1+z)H_\parallel}, \quad \frac{dr}{dz} = \frac{\sqrt{1 + \Omega_{K0}H_{\perp0}^2r^2}}{(1+z)\partial_t\partial_r(a_\perp r)}, \quad (86)$$

where the radial Hubble rate is $H_\parallel(t, r) = [\partial_t\partial_r(a_\perp r)]/[\partial_r(a_\perp r)]$. The area distance is then

$$D_A(z) = a_\perp(t(z), r(z))r(z). \quad (87)$$

3. Numerical investigation

We can compare these different approximations numerically. First consider the case of a single density fluctuation. Figure 4 shows the results of looking through a large void and large overdensity, 500 Mpc away, modelled with a Gaussian deviation from $\alpha = 1$ of width ~ 100 Mpc. An underdensity causes an increase in the distance modulus at redshifts beyond itself, in both the DR and modified DR cases; the opposite happens for an overdensity.

The DR and modified DR are qualitatively similar, while the shell approximation is very different. According to the (modified) DR approximations, we should expect SNIa to appear dimmer when located behind an underdensity as compared to an overdensity. By contrast, the shell approximation gives the opposite effect with a much larger amplitude: SNIa located behind a void appear *brighter* than in the fiducial cosmology; located behind an overdensity, they appear dimmer. The reason is as follows: although a void results in a negatively curved region (which would imply diverging light

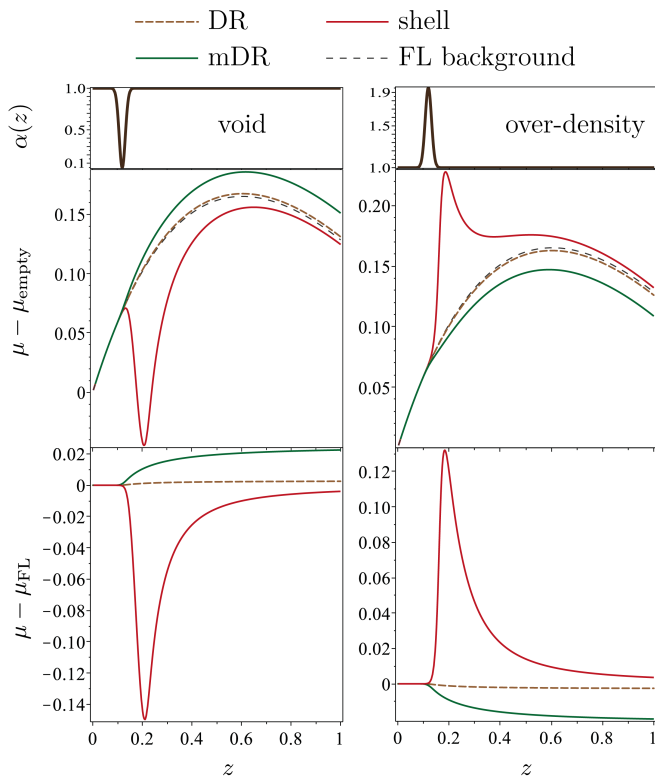


FIG. 4: The effect of a single void (left) or overdensity (right) on the distance modulus $\mu = 5 \log_{10}(D_L/10 \text{ pc})$ according to three different approximations, using as a ‘background’ a flat LCDM model with $\Omega_m = 0.25$, $h = 0.7$.

rays and larger distances), this is accompanied by an increase in the *expansion rate* in that region, which actually has a much stronger effect on distances (compare [69]). In FL, increasing the expansion rate and decreasing the density while keeping the age fixed results in a model with smaller distances, and this is exactly what happens here. For an overdensity, the reverse applies. However, note that while the shell approximation captures the mean expansion rate down the line of sight nicely, it may not capture the radial expansion rate correctly. E.g., looking through a spherical void vs a shell with the same density profile have different shear along the line of sight, making our approximation somewhat exaggerated in such a case.

Now consider the case where the density along the line of sight is reduced by a fixed percentage below the background value. Figure 3 shows that the main contribution of smoothing a simulation over smaller beam sizes is to reduce the mean value of α , since particles of significant size are rarely encountered. In the DR and modified DR approximations this amounts to fixing $\alpha = \text{const.}$ and Monte Carlo-ing over the PDF. In the shell approximation we have $\delta = \alpha - 1$ (since ρ is constant, this is really just an FL model with adjusted parameters). In Fig. 5 we show the distance modulus for two fiducial backgrounds: one a standard LCDM model, the other

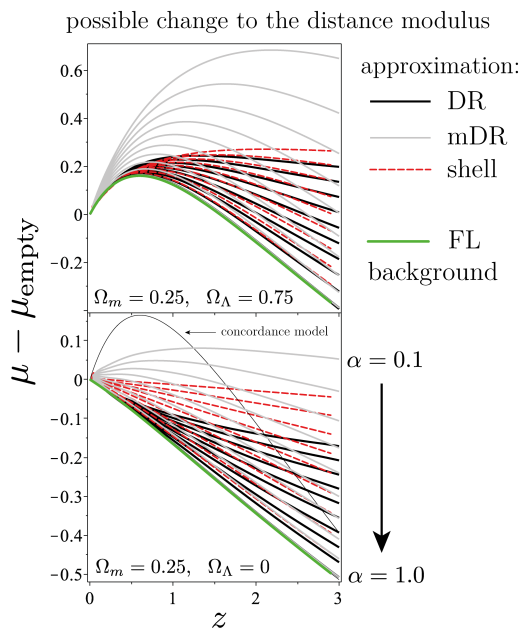


FIG. 5: We show the effect of differing mean values of α based on different approximations described in the text. The best known of these is the Dyer-Roeder (DR) which simply reduces the energy density in the light propagation equations while keeping the background expansion rate. Attempts to model this more accurately by accounting for the varying expansion rate encountered along the beam yield very different contributions depending on how this is modelled. One such modified DR (mDR) gives dark energy-like behaviour in the distance modulus even for a model with no cosmological constant (all shown compared to an empty model).

a curved CDM model with $\Lambda = 0$. We see that all the approximations give a systematic dimming effect to varying degrees. (There is actually an overall brightening in the shell case due to the change in h , but we have subtracted this off because SNIa observations are only sensitive to relative magnitudes, not absolute ones, which is marginalised over together with h .) While the DR and shell approximations are rather similar, giving changes to the distance modulus of at most 0.1 at $z \sim 1$, we see that the modified DR approximation gives a much stronger effect, of several times that.

It is striking that in the case $\Lambda = 0$ for $\alpha \lesssim 0.3$ we see the modified DR distance modulus mimicking the behaviour of a dark energy component. More specifically, both the DR and modified DR approximations can mimic a LCDM model, though the DR approximation requires a drastic change to α at low redshift to do so. For the modified DR approximation this is not so – see Fig. (6) – and it is well known that an LTB distance modulus can mimic any FL one.

It is clear from Fig. 4 that the DR approximation and plausible variations of it can give very different results – so that the basis of the DR approximation itself is sus-

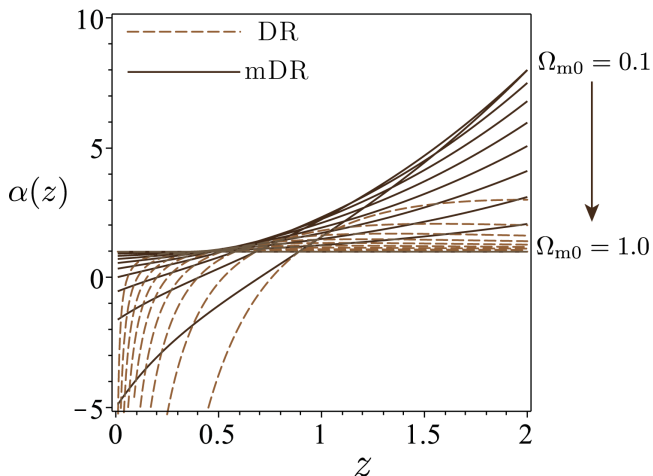


FIG. 6: The $\alpha(z)$ required to give a LCDM $D_A(z)$ curve, for a variety of Ω_{m0} (with curvature making up the rest of the energy component). The DR approximation requires extremely negative values of α to mimic dark energy, which might suggest that the effect of modelling narrow beams may not be important for dark energy, and certainly could not be the underlying cause of it. On the other hand, a simple modification to DR yields an approximation that much more readily produces dark energy-like effects. This suggests instead that modelling narrow beams properly, and getting the DR approximation right, could be vital for determining the nature of dark energy.

pect.

E. Other approaches

Other approaches to the problem of light propagation in a clumpy universe are based on exact nonlinear solutions or numerical methods or both.

In “Swiss cheese” models, an FL universe contains one or more spherical inhomogeneous regions, with the same average density as the FL model, which could be Schwarzschild vacuoles, or more realistically, LTB balls. These have been used extensively to model the effect of inhomogeneities on light rays (e.g. [89–97]). The results depend on the position and nature of the inhomogeneous regions, as well as on the method for randomization of light rays. A careful analysis that approximates observations in all directions and over a range of distances [97] concludes that there are only small corrections to the standard FL results. This is not surprising, since the average density along typical lines of sight is very close to the FL density. For the case of SNIa beams, which may preferentially sample underdense regions, the results could be different. However, an inherent limitation of this approach is that, by construction, and given the highly symmetric nature of the inhomogeneities, the clumps do not affect the expansion rate of the universe.

The method of ray-tracing through N-body simula-

tions (e.g. [98]) is very useful for statistical analysis and predictions for lensing observations. However, the dynamical range of scales of matter inhomogeneities that the simulations can reproduce is very limited. Ray-tracing within N-body simulations is usually done by projecting all matter onto equally spaced ‘lens planes’ which are separated by about 100 Mpc. Such an approach is not able to clarify the effect that halos below the simulations mass resolution have on light bundles from SNIa.

Exact solutions that are more general than the Swiss cheese models are usually less realistic, given the highly nonlinear nature of GR. A class of Szekeres models, in which inhomogeneities may be modelled as nonlinear perturbations on an FL background, has been used to investigate light propagation by [99]. Despite the idealized nature of clumping, the results show that for inhomogeneities of large spatial size, parameter estimation could be seriously affected (see also [100]). A stronger conclusion follows from analyzing light rays in a universe with regularly spaced point masses separated by vacuum [101]. The average dynamics is close to LCDM, but the optics behaves very differently. Unlike N-body simulations, this model is self-consistent (i.e. the particles generate their own spacetime geometry). However the modelling of matter is necessarily over-simplified.

V. RICCI AND WEYL FOCUSING

The DR approximation neglects the effect of point sources and the Weyl focusing they produce, in particular in the strong lensing regime where it is not negligible. This issue was addressed in [24], by considering the effect of the DR equation (for almost all directions, where Weyl effects can be neglected) and the effect of strong lensing (for the relatively few directions where lightrays pass close to matter, with strong lensing occurring and leading to multiple images). These combined effects are shown to lead to the usual FL relations when averaged over the whole sky, the decreased flux in most directions being compensated by higher flux in a few directions.

Keeping in mind that strong lensing effects are negligible in most directions, and in particular for most SNIa (unless we observe a galaxy or a cluster on the line of sight), we can try to go a step further than the DR approximation by relating, at least heuristically, the Weyl focusing to an effective Ricci focusing. The approximation that the SNIa bundles remain in the weak-field regime can be supported as follows. If matter is modelled as a gas of particles of mass m and proper radius r_* , with mean number density n , then the mean energy density is $\rho = mn$. The probability that a line of sight intersects such a matter particle within the redshift band $z \rightarrow z+dz$ is proportional to the surface area of the particles, to their density, and to the distance light propagates in this redshift interval, i.e.

$$dP = \pi r_*^2 n(z) \frac{dz}{(1+z)H(z)}. \quad (88)$$

The average number of particle intersections before the redshift z is the optical depth,

$$\tau(z) = \pi r_*^2 \int_0^z \frac{n(z')}{(1+z')H(z')} dz'. \quad (89)$$

We assume particle number conservation, $n(z) = n_0(1+z)^3$, with $n_0 \sim 0.005 h^3 \text{Mpc}^{-3}$ (number density of halos above $10^{12} h^{-1} M_\odot$ which comprise about 50% of the mass in the universe) and $r_* \sim 20 h^{-1} \text{kpc}$ for the central, high density, region of the halos where the galaxies are assumed to reside. This implies that at $z = 1$, $\tau \sim 0.023$ and $\tau = 0.032$, which means that only 2.3% and 3.2% of the lines of sight intersect a galaxy before $z = 1$, respectively for an Einstein-de Sitter and a flat Λ CDM model with $\Omega_m = 0.3$. This is a rough estimate – Λ and inhomogeneous distribution of the luminous matter would tend to lower it.

In order to describe the transition from Weyl to Ricci focusing, we first recall the lensing effect of a single mass, whose gravitational potential is

$$\Phi = -Gm(b^2 + u^2)^{-1/2}, \quad (90)$$

where b is the impact parameter and u the distance along the line of sight. The deflection angle is thus

$$\alpha = 4Gm \frac{b}{b^2}. \quad (91)$$

The critical density and the Einstein angular radius are respectively defined by $\Sigma_{\text{crit}} = D_{OS}/(4\pi G D_{OL} D_{LS})$ and $\theta_E^2 = 4Gm D_{LS}/(D_{OL} D_{OS})$, so that the lens equation takes the form

$$\theta = \theta_s + \hat{\alpha}(\theta), \quad (92)$$

where D_{LS} , D_{OL} and D_{OS} are the angular distances between the lens plane and the source, the observer and the lens plane, and the observer and the source. The angular position of the image on the lens plane is then given by $\theta = \mathbf{b}/D_{OL}$. $\hat{\alpha}$ is given by $\hat{\alpha} = \theta \theta_E^2/\theta^2$, since $\Sigma(\theta) = m\delta^{(2)}(\mathbf{b}) = m\delta^{(2)}(\theta)/D_{OL}^2$ for a point mass. The amplification matrix is then obtained as $\mathcal{A}_b^a = \partial\theta_s^a/\partial\theta^b$, so that $\mathcal{A}_{ab} = \delta_{ab} - \partial_{\theta^a}\hat{\alpha}_b = \delta_{ab} - \partial_{\theta^a}\partial_{\theta^b}\psi$ with

$$\psi = \theta_E^2 \ln \theta. \quad (93)$$

We conclude that the convergence and the shear are given by

$$\kappa = \pi\theta_E^2\delta^{(2)}(\theta), \quad (\gamma_1, \gamma_2) = \frac{\theta_E^2}{\theta^4}(\theta_2^2 - \theta_1^2, 2\theta_1\theta_2), \quad (94)$$

which is more easily written in terms of the polar angle on the screen ($\theta_1 = \theta \cos \varphi$, $\theta_2 = \theta \sin \varphi$) as

$$(\gamma_1, \gamma_2) = -\frac{\theta_E^2}{\theta^2}(\cos 2\varphi, \sin 2\varphi). \quad (95)$$

For a single mass and a line of sight that does not intersect it, $\kappa = 0$ and the magnification is $\mu = [1 -$

$|\gamma|^2]^{-1} \sim 1 + 2\theta_E^4\theta^{-4}$, neglecting the image inside the Einstein radius. Now consider a shell of thickness dz such that the density of particles is $n(z)$ and such that $d\chi \ll D_{LS}, D_{OL}, D_{OS}$. For a typical lightray the total amplification matrix will have a shear given by

$$[\hat{\gamma}_1(z), \hat{\gamma}_2(z)] = \theta_E^2 \sum \left[\frac{\cos 2\varphi}{\theta^2}, \frac{\sin 2\varphi}{\theta^2} \right], \quad (96)$$

where the sum is over all particles of the shell. If the particles are distributed homogeneously, this implies that they are isotropically distributed around the line of sight, so that we expect $\hat{\gamma}_1(z), \hat{\gamma}_2(z) \sim 0$.

Intuitively, this is understood by the fact that each point mass induces an ellipticity in a different direction and they should average to reduce the total ellipticity. The remaining effect of all the Weyl distortions is thus an effective convergence that can be determined from the magnification $\hat{\kappa}(z) = \theta_E^4 \sum \theta^{-4}$. Estimating the sum by assuming we have a uniform distribution and that the typical smallest distance is $\theta \sim n^{-1/3}/D_{OL}$, we get that $\sum \theta^{-4} \sim D_{OL}^3 n$, and thus

$$\hat{\kappa}(z) \sim f_K^3[\chi(z)]n(z) \left\{ 4Gm \frac{f_K[\chi(z_s) - \chi(z)]}{f_K[\chi(z)]f_K[\chi(z_s)]} \right\}^2, \quad (97)$$

where $f_K(\chi)$ is the unfilled angular distance, i.e. using \hat{H} instead of H in (61). We can compare to the effect that a homogeneous distribution of density $n_{\text{eff}}(z) = \alpha(z)n(z)$ would generate through its Ricci focusing to get

$$\alpha(z) = 4Gm \frac{f_K[\chi(z_s) - \chi(z)]}{f_K[\chi(z_s)]} H(z). \quad (98)$$

This is the effective DR parameter for the averaged Ricci convergence. It stills depend explicitly on m because this is a second order effect, hence scaling as θ_E^4 , while it is first order in a homogeneous medium. Such an estimate is indeed very crude but it confirms the statements of [24, 57] and the results of the numerical simulations of [41].

VI. DISCUSSION AND CONCLUSIONS

The effect of the inhomogeneity of the matter distribution induces a dispersion of the magnification of SNIa and thus of the luminosity distance. We have argued that this effect has not been properly modelled for SNIa since the beam is very narrow and far below the scales resolved in any numerical simulation.

For the first time, we have attempted to quantify the probability distribution for narrow beams, using a combination of N-body simulations and a PS approach. For a narrow beam of fixed length, the PDF is non-Gaussian, peaked at densities below the cosmic mean, with a power-law tail, whose power depends on the diameter of the beam, describing the relatively few lines of sight which have an over-dense mean. These PDFs contrast sharply

with distributions based on using cubes of the same volume. These estimations are based on current N-body simulations which do not have the resolution to probe beams with a diameter $\lesssim 100 h^{-1}$ kpc. Nevertheless, the trend is clear: narrow beams typically experience a lower than average density, and do not sample the cosmic mean density until their length approaches the Hubble scale. Based on our results, we estimate that significantly more than 75% of beams experience less than the mean density.

From a theoretical point of view, the effect must be described by the set of equations (21), (22) and (30) that describe the distortion and magnification of any light bundle, whatever the spacetime geometry. The explicit covariant form of these equations is given by (50)–(55). The main problem is that the solution of this set of equations requires a description of the distribution of matter on the scale of the beam size, i.e. on scales much smaller than those of our current understanding.

This dispersion has been modelled in some regimes but we argue that the distribution of matter on the scales relevant for the description of a SNIa bundle is not understood yet. On such small scales, the statistical dispersion comes with a bias that has two origins: (1) the fact that the nonlinear terms in the expression for the magnification can not be neglected a priori; (2) an observational selection effect due to the fact that most SNIa are observed in directions where they are not overshadowed by a galaxy. The bundles included in SNIa analysis are thus more likely to probe under-dense regions.

Why is the Hubble diagram so compatible with that of a Friedmann-Lemaître universe? In particular, the typical transverse size of the bundle is smaller than the typical mean distance between the smallest bound structures in the currently favoured Λ CDM paradigm. Why does the fluid approximation used to interpret the data hold? This question is two-sided. It questions the robustness of the interpretation of the cosmological data but also offers a way to constrain the distribution of matter on small scales. We also gave a heuristic argument concerning the Ricci-Weyl focusing issue, leading to a prediction of an effective DR factor $\alpha(z)$ once the fractions of clustered and smooth matter are known.

Another description is provided by the Dyer-Roeder equation. It has however some simplifying hypotheses that neglect the effects of changes in $v(z)$ and the local expansion due to clumping. We suggested two plausible modifications to the DR approach, and showed that the 3 models produce very different results – thus undermining confidence in the DR approximation. In particular, it is not clear whether under-densities lead to demagnification (due to negative curvature) or magnification (due to the increase in the expansion rate). Our shell approximation clearly points to the opposite effect calculated via normal lensing or the DR approximation: a SN located just behind an under-density should appear brighter than it would in the fiducial cosmology. In fact, we estimate that a SN the far side of a 100 Mpc void could be 0.1 mag brighter than it would be with not void present. Though

likely an over-estimation, this could have important implications for parameter estimation from SNIa. Quantifying this properly is an important open problem. In fact, it is striking to note from our investigations of N-body simulations that we should expect α to vary as a function of radius from us from significantly below unity locally, approaching unity only on Hubble scales. Within our shell approximation, this would give exactly the kind of model used in Hubble scale ‘void models’, which require no dark energy, but without any kind of anti-Copernican fine tuning involved [103]. Every observer would observe such an effect.

While accurate modelling of such beams may be problematic for some time, we can still observationally test to see if there are problems and phenomenologically correct for them.

SNIa line of sight Dividing up SNIa samples according to the estimated density along the line of sight may reveal a bias. If so, this may indicate that the effects we have discussed here must be taken into account.

discordant distances In any exact relativistic model the luminosity distance is $D_L = (1+z)^2 D_A$, where D_A is the area angular diameter distance. Large scale measurements of the area distance will not be affected by the problems we have discussed here, however, so we can expect a failure at some level of this relation when comparing measurements of D_A from large scale measurements such as the BAO and the CMB to measurements of D_L from SNIa. On smaller scales, where the area distance is measured from radio or quasar sources, there could be an effective reciprocity breakdown because such sources still have much larger beam sizes than SNIa, and so smear the matter distribution to include many more over-dense regions. Such a violation was found in [102], where a relative brightening of SNIa was found – as we would predict from the shell approximation.

consistency conditions A variety of consistency tests have recently been developed as a way of testing the standard model (see [103] for a review). It has recently been shown that these are strongly sensitive to changes of the DR form [104]. This implies that they can be used to probe the effects we have discussed here.

Generically, then, distances to the same object will depend on the scale over which the light from the source smears the intervening matter distribution.

We have found that the old problem of modelling narrow beams remains unsolved. As different interpretations of the problem give conflicting yet significant effects, we believe this problem needs considerably more attention. This is important not only from a theoretical perspective, but to ensure precision cosmology delivers correct answers as well as precise ones.

Acknowledgements:

We thank David Bacon, Krzysztof Bolejko, Peter Coles, Ruth Durrer, Stefan Hilbert, Yannick Mellier, Bob Nichol, Brian Schmidt, Joe Silk, Zachary Slepian and Yun Wang for discussions and/or comments. RM is supported by a South African SKA Research Chair, and by the UK Science & Technology Facilities Council (grant no. ST/H002774/1). CC, GE, AF, RM, OU are supported by a NRF (South Africa)/ Royal Society (UK) exchange grant. JPU is partially supported by the ANR-Thales. The Millennium Simulation and the MultiDark

databases used in this paper and the web application providing online access to them were constructed as part of the activities of the German Astrophysical Virtual Observatory. Data for halos and galaxies are publicly available at <http://www.mpa-garching.mpg.de/millennium> and <http://www.multidark.org/MultiDark>. The MultiDark database is the result of a collaboration between the Leibniz-Institute for Astrophysics Potsdam (AIP) and the Spanish MultiDark Consolider Project CSD2009-00064. The Bolshoi and MultiDark simulations were run on the NASA's Pleiades supercomputer at the NASA Ames Research Center.

-
- [1] R. Amanullah *et al.*, “Spectra and Light Curves of Six Type Ia Supernovae at $0.511 < z < 1.12$ and the Union2 Compilation,” *Astrophys. J.* **716**, 712 (2010) [arXiv:1004.1711].
 - [2] Ya. B. Zel’dovich, “Observations in a universe homogeneous in the mean”, *Soviet Astr. AJ* **8**, 13 (1964).
 - [3] R. P. Feynman, unpublished talk (1964). (See [6].)
 - [4] V. M. Dashevskii and V. I. Slysh, “On the Propagation of Light in a Nonhomogeneous Universe”, *Soviet Astr. AJ* **9**, 671 (1966).
 - [5] B. Bertotti, “The luminosity of distant galaxies,” *Proc. Roy. Soc. (London) A* **294**, 195 (1966).
 - [6] J. E. Gunn, “A fundamental limitation on the accuracy of angular measurements in observational cosmology”, *Astrophys. J.* **147**, 61 (1967); J. E. Gunn, “On the propagation of light in inhomogeneous cosmologies. I. Mean effects”, *Astrophys. J.* **150**, 737 (1967).
 - [7] R. Kantowski, “Corrections in the luminosity-redshift relations of the homogeneous Friedmann models”, *Astrophys. J.* **155**, 89 (1969).
 - [8] S. Refsdal, “On the propagation of light in universes with inhomogeneous mass distribution”, *Astrophys. J.* **159**, 357 (1970).
 - [9] R. Kantowski, T. Vaughan and D. Branch, “The Effects of Inhomogeneities on Evaluating the Deceleration Parameter q_0 ,” *Astrophys. J.* **447**, 35 (1995) [arXiv:astro-ph/9511108].
 - [10] J.A. Frieman, “Weak Lensing and the Measurement of q_0 from Type Ia Supernovae”, *Comm. Astrophys.* **18**, 323 (1998) [astro-ph/9608068].
 - [11] Y. Wang, “Supernova pencil beam survey,” *Astrophys. J.* **531**, 676 (2000) [astro-ph/9806185].
 - [12] Y. Wang, “Flux-averaging analysis of type ia supernova data,” *Astrophys. J.* **536**, 531 (2000) [astro-ph/9907405].
 - [13] Y. Wang, “Evidence for weak lensing of supernovae,” *JCAP* **0503**, 005 (2005) [astro-ph/0406635].
 - [14] D. E. Holz and E. V. Linder, “Safety in numbers: Gravitational Lensing Degradation of the Luminosity Distance-Redshift Relation,” *Astrophys. J.* **631**, 678 (2005) [arXiv:astro-ph/0412173].
 - [15] A. Cooray, D. Holz and D. Huterer, “Cosmology from supernova magnification maps,” *Astrophys. J.* **637**, L77 (2006) [arXiv:astro-ph/0509579].
 - [16] S. Dodelson and A. Vallinotto, “Learning from the Scatter in Type Ia Supernovae,” *Phys. Rev. D* **74**, 063515 (2006) [arXiv:astro-ph/0511086].
 - [17] C. Shapiro, D. Bacon, M. Hendry and B. Hoyle, “Delensing Gravitational Wave Standard Sirens with Shear and Flexion Maps,” *Mon. Not. Roy. Astron. Soc.* **404**, 858 (2010) [arXiv:0907.3635]; C. M. Hirata, D. E. Holz and C. Cutler, “Reducing the weak lensing noise for the gravitational wave Hubble diagram using the non-Gaussianity of the magnification distribution,” *Phys. Rev. D* **81**, 124046 (2010) [arXiv:1004.3988].
 - [18] N. Dalal, D. E. Holz, X. I. Chen and J. A. Frieman, “Corrective lenses for high redshift Supernovae,” *Astrophys. J.* **585**, L11 (2003) [arXiv:astro-ph/0206339].
 - [19] F. Bernardeau, “Weak lensing detection in CMB maps”, *Astron. Astrophys.* **324**, 15 (1997)
 - [20] Y. Mellier, “Probing the Universe with Weak Lensing,” *Ann. Rev. Astron. Astrophys.* **37** (1999) 127, [arXiv:astro-ph/9812172].
 - [21] B. Jain and U. Seljak, “Cosmological model predictions for weak lensing: Linear and nonlinear regimes”, *Astrophys. J.* **484**, 560 (1997) [arXiv:astro-ph/9611077].
 - [22] K. Kainulainen and V. Marra, “SNe observations in a meatball universe with a local void,” *Phys. Rev. D* **80**, 127301 (2009) [arXiv:0906.3871].
 - [23] K. Kainulainen and V. Marra, “Accurate Modeling of Weak Lensing with the sGL Method,” *Phys. Rev. D* **83**, 023009 (2011) [arXiv:1011.0732].
 - [24] S. Weinberg, “Apparent luminosities in a locally inhomogeneous universe,” *Astrophys. J.* **208**, L1 (1976).
 - [25] W. P. Press and P. Schechter, “Formation of Galaxies and Clusters of Galaxies by Self-Similar Gravitational Condensation”, *Astrophys. J.* **187**, 425 (1974).
 - [26] A. Jenkins, C. S. Frenk, S. D. M. White, J. M. Colberg, S. Cole, A. E. Evrard, H. M. P. Couchman and N. Yoshida, “The mass function of dark matter haloes”, *Mon. Not. Roy. Astron. Soc.* **321**, 372 (2001) [arXiv:astro-ph/0005260].
 - [27] D. Reed, J. Gardner, T. Quinn, J. Stadel, M. Fardal, G. Lake and F. Governato, “Evolution of the mass function of dark matter haloes”, *Mon. Not. Roy. Astron. Soc.* **346**, 565 (2003) [arXiv:astro-ph/0301270].
 - [28] M. S. Warren, K. Abazajian, D. E. Holz and L. Teodoro, “Precision Determination of the Mass Function of Dark Matter Halos”, *Astrophys. J.* **646**, 881 (2006) [arXiv:astro-ph/0506395].
 - [29] D. S. Reed, R. Bower, C. S. Frenk, A. Jenkins and T. Theuns, “The halo mass function from the dark ages

- through the present day”, *Mon. Not. Roy. Astron. Soc.* **374**, 2 (2007) [arXiv:astro-ph/0607150].
- [30] J. Tinker, A. V. Kravtsov, A. Klypin, K. Abazajian, M. Warren, G. Yepes, S. Gottlber, and D. E. Holz, “Toward a Halo Mass Function for Precision Cosmology: The Limits of Universality”, *Astrophys. J.* **688**, 709 (2008) [arXiv:0803.2706].
- [31] D. Anderhalden and J. Diemand, “The total mass of dark matter haloes”, *Mon. Not. Roy. Astron. Soc.* **414**, 3166 (2011) [arXiv:1102.5736].
- [32] A. Faltenbacher, A. Finoguenov and N. Drory, “The Halo Mass Function Conditioned on Density from the Millennium Simulation”, *Astrophys. J.* **712**, 484 (2010) [arXiv:1002.0844].
- [33] S. More, A. V. Kravtsov, N. Dalal and S. Gottlber, “The overdensity and masses of the friends-of-friends halos and universality of the halo mass function”, [arXiv:1103.0005].
- [34] F. Prada, A. Klypin, E. Simonneau, J. Betancort-Rijo, S. Patiri, S. Gottlöber, S. and M. A. Sanchez-Conde, “How Far Do They Go? The Outer Structure of Galactic Dark Matter Halos”, *Astrophys. J.* **645**, 1001 (2006) [arXiv:astro-ph/0506432].
- [35] A. J. Cuesta, F. Prada, A. Klypin and M. Moles, “The virialized mass of dark matter haloes”, *Mon. Not. Roy. Astron. Soc.* **389**, 385 (2008) [arXiv:0710.5520].
- [36] E. Komatsu, J. Dunkley, M. R.olta et al. “Five-Year Wilkinson Microwave Anisotropy Probe Observations: Cosmological Interpretation”, *ApJS* **180**, 330 (2009) [arXiv:0803.0547].
- [37] R. B. Metcalf and J. Silk, “A fundamental test of the nature of dark matter”, *Astrophys. J.* **519**, L1 (1999) [arXiv:astro-ph/9708036].
- [38] R. B. Metcalf and J. Silk, “New Constraints on Macroscopic Compact Objects as a Dark Matter Candidate from Gravitational Lensing of Type Ia Supernovae”, *Phys. Rev. Lett.* **98**, 071302 (2007) [arXiv:astro-ph/0612253].
- [39] P. Schneider, and R.V. Wagoner, “Amplification and polarization of Supernovae by gravitational lensing”, *Astrophys. J.* **314**, 154 (1987).
- [40] K.P. Rauch, “Gravitational microlensing of high-redshift Supernovae by compact objects”, *Astrophys. J.* **374**, 83 (1991).
- [41] D. E. Holz and R. M. Wald, “A New method for determining cumulative gravitational lensing effects in inhomogeneous universes”, *Phys. Rev. D* **58**, 063501 (1998) [arXiv:astro-ph/9708036].
- [42] U. Seljak, and D.E. Holz, “Limits on the density of compact objects from high redshift Supernovae”, *Astron. Astrophys. Lett.* **351**, L10 (1999) [astro-ph/9910482].
- [43] G. Bertone, D. Hooper and J. Silk, “Particle dark matter: evidence, candidates and constraints”, *Phys. Rep.* **405**, 279 (2005) [arXiv:hep-ph/0404175].
- [44] J. Diemand, B. Moore and J. Stadel, “Earth-mass dark-matter haloes as the first structures in the early Universe”, *Nature* **433**, 389 (2005) [arXiv:astro-ph/0501589].
- [45] A. R. Zentner, “The Excursion Set Theory of Halo Mass Functions, Halo Clustering, and Halo Growth”, *Int. J. Mod. Phys. D* **16** 763 (2007) [arXiv:astro-ph/0611454].
- [46] R. E. Angulo and S. D. M. White, “The birth and growth of neutralino haloes”, *Mon. Not. Roy. Astron. Soc.* **401**, 1796 (2010) [arXiv:0906.1730].
- [47] A. A. Klypin, S. Trujillo-Gomez, S. Primack, “Dark Matter Halos in the Standard Cosmological Model: Results from the Bolshoi Simulation” *ApJ* **740**, 102 (2011) [arXiv:1002.3660].
- [48] V. Springel, S. D. M. White, A. Jenkins et al., “Simulations of the formation, evolution and clustering of galaxies and quasars” *Nature* **435**, 629 (2005) [arXiv:astro-ph/0504097].
- [49] F. Prada, A. A. Klypin, A. Cuesta et al., “Halo concentrations in the standard LCDM cosmology” [arXiv:1104.5130].
- [50] G. Lemson & Virgo Consortium, “Halo and Galaxy Formation Histories from the Millennium Simulation: Public release of a VO-oriented and SQL-queryable database for studying the evolution of galaxies in the LambdaCDM cosmogony” [arXiv:astro-ph/0608019].
- [51] K. Riebe, A. Partl, H. Enke et al., “The MultiDark Database: Release of the Bolshoi and MultiDark Cosmological Simulations” [arXiv:1109.0003].
- [52] S. Masaki, M. Fukugita and N. Yoshida, “Matter Distribution around Galaxies,” [arXiv:1105.3005].
- [53] R. Sachs, Gravitational waves in General Relativity. VI. The outgoing radiation condition”, *Proc. Roy. Soc. Lond. A* **264**, 309 (1961).
- [54] C. C. Dyer, and R. C. Roeder, “The distance-redshift relation for universes with no intergalactic medium,” *Astrophys. J.* **174**, L115 (1972).
- [55] C. C. Dyer, and R. C. Roeder, “Distance-redshift relations for universes with some intergalactic medium,” *Astrophys. J.* **180**, L31 (1973).
- [56] C. C. Dyer, and R. C. Roeder, “Observations in locally inhomogeneous cosmological models,” *Astrophys. J.* **189**, 167 (1974).
- [57] C.C. Dyer, and R.C. Roeder, “On the transition from Weyl to Ricci focusing,” *Gen. Relat. Grav.* **13**, 1157 (1981).
- [58] L. Fang and X. Wu, “Geometrical optics in an inhomogeneous universe”, *Chinese. Phys. Lett.* **6**, 223 (1989); X. Wu, “The magnitude-redshift relation in a locally inhomogeneous universe”, *Astron. Astrophys.* **239**, 29 (1990).
- [59] G. F. R. Ellis, B. A. Bassett and P. K. S. Dunsby, “Lensing and caustic effects on cosmological distances,” *Class. Quant. Grav.* **15**, 2345 (1998) [arXiv:gr-qc/9801092].
- [60] H. G. Rose, “Apparent magnitudes in an inhomogeneous universe: The Global viewpoint,” *Astrophys. J.* **560**, L15 (2001) [arXiv:astro-ph/0106489].
- [61] T. W. B. Kibble and R. Lieu, “Average magnification effect of clumping of matter,” *Astrophys. J.* **632**, 718 (2005) [arXiv:astro-ph/0412275].
- [62] V. Kostov, “Average luminosity distance in inhomogeneous universes,” *JCAP* **1004**, 001 (2010) [arXiv:0910.2611].
- [63] C. Pitrou, T. Pereira, and J.-P. Uzan, “Weak lensing B-modes on all scales as a probe of local isotropy”, [arXiv:1204.1203.6029].
- [64] C. Clarkson and R. Maartens, “Inhomogeneity and the foundations of concordance cosmology,” *Class. Quant. Grav.* **27**, 124008 (2010) [arXiv:1005.2165].
- [65] C. Clarkson, R. Durrer, R. Maartens and O. Umeh, in preparation.
- [66] C. G. Tsagas, A. Challinor and R. Maartens, “Relativistic cosmology and large-scale structure,” *Phys. Rept.* **465**, 61 (2008) [arXiv:0705.4397].

- [67] M. Sasaki, “Cosmological gravitational lens equation: its validity and limitation”, *Prog. Theor. Phys.* **90**, 753 (1993).
- [68] K. Tomita, H. Asada and T. Hamana, “Distances in inhomogeneous cosmological models,” *Prog. Theor. Phys. Suppl.* **133**, 155 (1999) [arXiv:astro-ph/9904351].
- [69] S. Rasanen, “Light propagation in statistically homogeneous and isotropic dust universes,” *JCAP* **0902**, 011 (2009) [arXiv:0812.2872].
- [70] S. Rasanen, “Light propagation in statistically homogeneous and isotropic universes with general matter content,” *JCAP* **1003**, 018 (2010) [arXiv:0912.3370].
- [71] P. Schneider, J. Ehlers, and E. E. Falco, *Gravitational Lenses* (Springer, 1992).
- [72] P. Peter and J.-P. Uzan, *Primordial cosmology* (Oxford Univ. Press, 2009).
- [73] V. Perlick, “Gravitational lensing from a spacetime perspective,” *Living Rev. Rel.* **7**, 9 (2004).
- [74] C. Bonvin, R. Durrer and M. A. Gasparini, “Fluctuations of the luminosity distance,” *Phys. Rev. D* **73**, 023523 (2006) [arXiv:astro-ph/0511183].
- [75] J.-P. Uzan, F. Bernardeau, and Y. Mellier, “Time drift of cosmological redshifts and its variance,” *Phys. Rev. D* **77** 021301(R) (2008) [arXiv:0711.1950].
- [76] A. Cooray, D. Huterer and D. Holz, “Problems with Pencils: Lensing Covariance of Supernova Distance Measurements,” *Phys. Rev. Lett.* **96**, 021301 (2006) [arXiv:astro-ph/0509581].
- [77] D. Sarkar, A. Amblard, D. E. Holz and A. Cooray, “Lensing and Supernovae: Quantifying The Bias on the Dark Energy Equation of State,” [arXiv:0710.4143].
- [78] A. R. Cooray, D. E. Holz and R. Caldwell, “Measuring dark energy spatial inhomogeneity with supernova data,” *JCAP* **1011**, 015 (2010) [arXiv:0812.0376].
- [79] A. Vallinotto, S. Dodelson and P. Zhang, “Magnification as a Tool in Weak Lensing,” [arXiv:1009.5590].
- [80] B. Ménard *et al.*, “Improving the accuracy of cosmic magnification statistics”, *Astron. Astrophys.* **403**, 817 (2003) [arXiv:astro-ph/0210112].
- [81] J. Ehlers and P. Schneider, “Self-consistent probabilities for gravitational lensing in inhomogeneous universes”, *Astron. Astrophys.* **168**, 57 (1986).
- [82] E.V. Linder, “Light propagation in generalized Friedmann universes”, *Astron. Astrophys.* **206**, 190 (1988).
- [83] K. Tomita, “Angular Diameter Distances in Clumpy Friedmann Universes”, *Prog. Theor. Phys.* **100**, 79 (1998) [astro-ph/9806047].
- [84] E. Mortsell, “The Dyer–Roeder distance-redshift relation in inhomogeneous universes,” [arXiv:astro-ph/0109197].
- [85] K. Bolejko, “Weak lensing and the Dyer–Roeder approximation,” *Mon. Not. Roy. Astron. Soc.* **412** 1937 (2011) [arXiv:1011.3876].
- [86] Y. Wang, C. -H. Chuang, P. Mukherjee, “A Comparative Study of Dark Energy Constraints from Current Observational Data,” [arXiv:1109.3172].
- [87] T. Mattsson, “Dark energy as a mirage,” *Gen. Rel. Grav.* **42**, 567-599 (2010) [arXiv:0711.4264].
- [88] S. February, J. Larena, M. Smith and C. Clarkson, “Rendering dark energy void”, *Mon. Not. Roy. Astron. Soc.* **405**, 2231 (2010) [arXiv:0909.1479].
- [89] N. Brouzakis, N. Tetradis and E. Tzavara, “The Effect of Large-Scale Inhomogeneities on the Luminosity Distance,” *JCAP* **0702**, 013 (2007) [arXiv:astro-ph/0612179]; N. Brouzakis, N. Tetradis and E. Tzavara, “Light Propagation and Large-Scale Inhomogeneities,” *JCAP* **0804**, 008 (2008) [arXiv:astro-ph/0703586].
- [90] T. Biswas and A. Notari, “Swiss-Cheese Inhomogeneous Cosmology and the Dark Energy Problem,” *JCAP* **0806**, 021 (2008) [arXiv:astro-ph/0702555].
- [91] V. Marra, E. W. Kolb, S. Matarrese and A. Riotto, “On cosmological observables in a swiss-cheese universe,” *Phys. Rev. D* **76**, 123004 (2007) [arXiv:0708.3622].
- [92] R. A. Vanderveld, E. E. Flanagan and I. Wasserman, “Luminosity distance in ‘Swiss cheese’ cosmology with randomized voids: I. Single void size,” *Phys. Rev. D* **78**, 083511 (2008) [arXiv:0808.1080].
- [93] T. Clifton and J. Zuntz, “Hubble Diagram Dispersion From Large-Scale Structure,” [arXiv:0902.0726].
- [94] W. Valkenburg, “Swiss Cheese and a Cheesy CMB,” *JCAP* **0906**, 010 (2009) [arXiv:0902.4698].
- [95] R. Kantowski, B. Chen and X. Dai, “Gravitational Lensing Corrections in Flat Λ CDM Cosmology,” *Astrophys. J.* **718**, 913 (2010) [arXiv:0909.3308].
- [96] K. Bolejko, M. -N. Celerier, “Szekeres Swiss-Cheese model and supernova observations,” *Phys. Rev.* **D82**, 103510 (2010) [arXiv:1005.2584].
- [97] S. J. Szybka, “On light propagation in Swiss-Cheese cosmologies,” *Phys. Rev.* **D84**, 044011 (2011) [arXiv:1012.5239].
- [98] R. Takahashi, M. Oguri, M. Sato and T. Hamana, “Probability Distribution Functions of Cosmological Lensing: Convergence, Shear, and Magnification,” [arXiv:1106.3823]; S. Hilbert, J. R. Gair, L. J. King, “Reducing distance errors for standard candles and standard sirens with weak-lensing shear and flexion maps,” *Mon. Not. Roy. Astron. Soc.* **412**, 1023 (2011) [arXiv:1007.2468]; S. Hilbert, S. D. M. White, J. Hartlap, P. Schneider, “Strong lensing optical depths in a Λ CDM universe,” *Mon. Not. Roy. Astron. Soc.* **382**, 121 (2007) [arXiv:astro-ph/0703803].
- [99] N. Meures and M. Bruni, “Redshift and distances in a Λ CDM cosmology with nonlinear inhomogeneities,” [arXiv:1107.4433].
- [100] A. Krasinski, K. Bolejko, “Redshift propagation equations in the $\beta' \neq 0$ Szekeres models,” *Phys. Rev.* **D83**, 083503 (2011) [arXiv:1007.2083].
- [101] T. Clifton and P. G. Ferreira, “Archipelagian Cosmology: Dynamics and Observables in a Universe with Discretized Matter Content,” *Phys. Rev. D* **80**, 103503 (2009) [arXiv:0907.4109]; T. Clifton, P. G. Ferreira, “Errors in Estimating Ω_Λ due to the Fluid Approximation,” *JCAP* **0910**, 026 (2009) [arXiv:0908.4488].
- [102] B. A. Bassett, M. Kunz, “Cosmic distance-duality as a probe of exotic physics and acceleration,” *Phys. Rev.* **D69**, 101305 (2004). [astro-ph/0312443].
- [103] C. Clarkson, Establishing homogeneity of the universe in the shadow of dark energy. [arXiv:1204.5505].
- [104] V. C. Busti and J. A. S. Lima, Cosmological Tests Plagued by Small-Scale Inhomogeneities. [arXiv:1204.1083].